Suppression of *Sproutys* Has a Therapeutic Effect for a Mouse Model of Ischemia by Enhancing Angiogenesis

Koji Taniguchi[1,2,3], Ken-ichiro Sasaki[4], Kousuke Watari[5], Hideo Yasukawa[4], Tsutomu Imaizumi[4], Toranoshin Ayada[1], Fuyuki Okamoto[1], Takuma Ishizaki[3], Reiko Kato[1], Ri-ichiro Kohno[6], Hiroshi Kimura[7], Yasufumi Sato[7], Mayumi Ono[5], Yoshikazu Yonemitsu[6,8], Akihiko Yoshimura[3,9]*

1 Division of Molecular and Cellular Immunology, Medical Institute of Bioregulation, Kyushu University, Fukuoka, Japan, **2** Department of Surgery and Science, Graduate School of Medical Sciences, Kyushu University, Fukuoka, Japan, **3** Department of Microbiology and Immunology, Keio University School of Medicine, Shinjuku-ku, Tokyo, Japan, **4** Division of Cardiovascular Medicine, Department of Internal Medicine, Kurume University, Kurume, Japan, **5** Department of Pharmaceutical Oncology, Graduate School of Pharmaceutical Sciences, Kyushu University, Fukuoka, Japan, **6** Division of Pathophysiological and Experimental Pathology, Department of Pathology, Graduate School of Medical Sciences, Kyushu University, Fukuoka, Japan, **7** Department of Vascular Biology, Institute of Development, Aging, and Cancer, Tohoku University, Sendai, Japan, **8** Department of Gene Therapy, Chiba University Graduate School of Medicine, Chiba, Japan, **9** Japan Science and Technology Corporation (JST), CREST, Kawaguchi, Japan

Abstract

Sprouty proteins (Sproutys) inhibit receptor tyrosine kinase signaling and control various aspects of branching morphogenesis. In this study, we examined the physiological function of Sproutys in angiogenesis, using gene targeting and short-hairpin RNA (shRNA) knockdown strategies. *Sprouty2* and *Sprouty4* double knockout (KO) (DKO) mice were embryonic-lethal around E12.5 due to cardiovascular defects. The number of peripheral blood vessels, but not that of lymphatic vessels, was increased in *Sprouty4* KO mice compared with wild-type (WT) mice. *Sprouty4* KO mice were more resistant to hind limb ischemia and soft tissue ischemia than WT mice were, because *Sprouty4* deficiency causes accelerated neovascularization. Moreover, suppression of *Sprouty2* and *Sprouty4* expression *in vivo* by shRNA targeting accelerated angiogenesis and has a therapeutic effect in a mouse model of hind limb ischemia. These data suggest that Sproutys are physiologically important negative regulators of angiogenesis *in vivo* and novel therapeutic targets for treating peripheral ischemic diseases.

Citation: Taniguchi K, Sasaki K-i, Watari K, Yasukawa H, Imaizumi T, et al. (2009) Suppression of *Sproutys* Has a Therapeutic Effect for a Mouse Model of Ischemia by Enhancing Angiogenesis. PLoS ONE 4(5): e5467. doi:10.1371/journal.pone.0005467

Editor: Rory Edward Morty, University of Giessen Lung Center, Germany

Received March 5, 2009; **Accepted** April 13, 2009; **Published** May 8, 2009

Funding: This study was supported by Grants-in-Aid for Scientific Research (S) and for Scientific Research on Priority Areas from the Ministry of Education, Culture, Sports, Science and Technology of Japan, the Program for Promotion of Fundamental Studies in Health Sciences of the National Institute of Biomedical Innovation (NIBIO), the Naito Foundation, and the Astellas Foundation for Research on Metabolic Disorders. The funders had no role in study design, data collection and analysis, decision to publish, or preparation of the manuscript.

Competing Interests: The authors have declared that no competing interests exist.

* E-mail: yoshimura@a6.keio.jp

Introduction

Growth factor-induced signaling by receptor tyrosine kinases (RTKs) plays several essential roles in development and pathogenesis; accordingly, it is tightly controlled by a number of regulatory proteins [1–3]. When a ligand binds to an RTK and recruits a Grb2-Sos to the inner surface of a membrane, the Sos protein binds to Ras, causing GDP/GTP exchange and thus activating Ras. Activated Ras recruits Raf to the plasma membrane and activates the Raf/MEK/extracellular signal-regulated kinase (ERK) pathway. Some growth factors, such as vascular endothelial growth factor (VEGF)-A, also activate the Raf/MEK/ERK pathway through the RTK/phospholipase C (PLC)-γ/protein kinase C (PKC) pathway, which is a Ras-independent pathway [4].

Sprouty (Spry) has been genetically identified as an antagonist of fibroblast growth factor (FGF) receptor in tracheal development in *Drosophila*, and is a proven negative regulator of the Ras/Raf/ERK pathway [5,6]. Four mammalian genes with sequence similarity to *Drosophila Sprouty* (*Sprouty1–4*) have been identified [1,2]. In addition, we have identified three Sprouty-related proteins known as Spred1–3 (Spreds), in which the C-terminal cysteine-rich domain found in Sprouty proteins (Sproutys) is conserved [7,8]. Since loss-of-function mutations of the *SPRED1* gene have been found in human neuro-cardio-facial-cutaneous (NCFC) syndromes [9], and since these syndromes are caused by dysregulation of the Ras-ERK pathway, we conclude that SPRED1 is a negative regulator of RTK-mediated Ras/ERK activation.

In the development of the cardiovascular system of *Drosophila*, as in the tracheal system, the formation of new blood vessels from preexisting ones (angiogenesis) involves the sprouting of endothelial cells out of an epithelial layer and the branching of tubular structures [10]. In the adult, angiogenesis only takes place during the female reproductive cycle, during wound healing, and in pathological situations, including tumor growth, diabetic retinopathy, arthritis, atherosclerosis, and psoriasis [10,11]. Angiogenesis is tightly regulated by a balance between inducing and inhibitory signals [12]. Growth factors, such as VEGF-A, basic FGF (bFGF), and angiopoietins, positively regulate angiogenesis by binding to

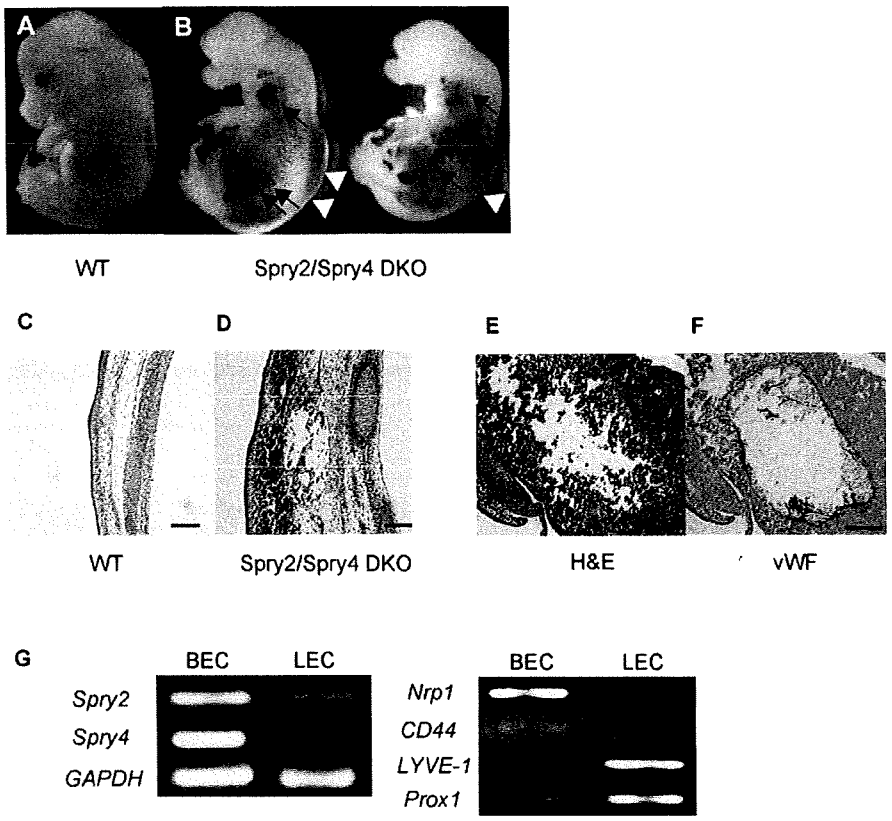

Figure 1. Characterization of *Sprouty2/Sprouty4* DKO mice. (A, B) Gross appearance of wild-type (WT) (A) and *Sprouty2/Sprouty4* DKO (B) embryos at embryonic day 12.5. The arrow and arrowheads indicate hemorrhage and edema, respectively. (C, D) Hematoxylin-eosin (H&E) staining of sections of WT (C) and *Sprouty2/Sprouty4* DKO (D) skin. (E, F) H&E staining and immunohistochemical staining with von Willebrand factor (vWF) of sections of hepatic hemangiomas in *Sprouty2/Sprouty4* DKO liver. vWF was used as a blood vessel marker. (G) Expression of *Sproutys* in endothelial cells. About 5.0×10^4 BECs and LECs were FACS-sorted at embryonic day 14.5, and were used for RT-PCR analysis. *GAPDH* served as a loading control. Good separation of BECs and LECs was confirmed by BEC markers (*Nrp1*, *CD44*) and LEC markers (*LYVE1*, *Prox1*). Scale bars (C–F): 100 μm.
doi:10.1371/journal.pone.0005467.g001

their cognate RTKs and thus inducing endothelial cell proliferation, migration, differentiation, and survival [12,13]. In addition, sphingosine-1-phosphate (S1P), which activates GPCRs, has also been implicated in angiogenesis [14]. In contrast, proteins that negatively regulate angiogenesis by specifically blocking RTK signaling are less well characterized.

Previous studies have demonstrated that overexpression of Sproutys inhibits VEGF-A- and bFGF-induced endothelial cell proliferation and differentiation *in vitro* as well as branching and sprouting of small vessels *in vivo* [15,16]. Moreover, Sprouty4 suppresses VEGF-A/VEGF receptor (VEGFR)-2 signaling *in vitro* [17–19]. We also know that Spreds, in contrast, inhibit VEGF-C signaling, which is important in lymphangiogenesis, and that *Spred1/Spred2* double knockout (KO) (DKO) mice show abnormal lymphatic development [18]. Yet the physiological role of Sproutys in angiogenesis and lymphangiogenesis remains to be elucidated.

In this study we investigated the physiological function of Sproutys in angiogenesis by performing knockout and knockdown analyses of *Sproutys*. We showed that Sproutys are negative regulators for angiogenesis rather than lymphangiogenesis *in vivo*. Moreover, *Sprouty4* KO mice were more resistant to hind limb ischemia and soft tissue ischemia than wild-type (WT) mice were, and *in vivo* shRNA targeting *Sprouty2* and *Sprouty4* accelerated angiogenesis in a mouse model of hind limb ischemia. These data suggest that Sprouty2 and Sprouty4 are important negative regulators of angiogenesis *in vivo* that could be new therapeutic targets for ischemic diseases.

Results

Increased developmental angiogenesis in *Sprouty*-deficient mice

Overexpression studies suggest that Sprouty2 and Sprouty4 possess similar negative effects on RTK-mediated ERK activation [20]. To define the overlapping functions of Sprouty2 and Sprouty4, we generated *Sprouty2/Sprouty4* DKO mice. *Sprouty2/Sprouty4* DKO mice were embryonic-lethal by embryonic day 12.5 and showed very severe defects in craniofacial and limb morphogenesis [21]. They also showed very severe subcutaneous hemorrhage, edema (Fig. 1A–D), and multiple hepatic hemangiomas (Fig. 1E,F), which suggested that they had cardiovascular defects as well. We next investigated the expression pattern of *Sprouty2* and *Sprouty4* in endothelial cells during embryonic development, and found that *Sprouty2* and *Sprouty4* were more highly expressed in blood endothelial cells (BECs) than in lymphatic endothelial cells (LECs) (Fig. 1G).

This discovery led us to examine vascularization in adult *Sprouty4* single KO mice in detail, although *Sprouty4* single KO

mice showed no obvious vascular phenotype [21]. *Sprouty4* single KO mice exhibited more vascular networks of blood vessels in the ear than WT mice did (Fig. 2A,B). Similarly, more vascular networks of blood vessels in the ear were observed in *Sprouty2* single KO mice than in WT mice (data not shown). The numbers of blood vessels in the skin were also increased in *Sprouty4* KO mice (Fig. 2C,D). Lymphatic vessel networks, on the other hand, were present at the same frequency in these *Sprouty4* KO mice as in WT mice (Fig. 2A–D). Retinal vasculature is a good model system for the study of general blood vessel development [22]. Vascular development in the early embryo is difficult to observe, but the murine retinal vascular system develops after birth and is therefore easier to examine. We compared flat-mounted retinas from WT and *Sprouty4* KO mice at postnatal day (PD) 3 after injecting FITC-dextran (Fig. 2E). As the image clearly shows, retinal angiogenesis was enhanced in *Sprouty4* KO mice compared to WT mice.

These data suggest that, in contrast to Spred1 and Spred2, which are important negative regulators of developmental lymphangiogenesis rather than developmental angiogenesis, as previously reported [18], Sprouty2 and Sprouty4 are important negative regulators of developmental angiogenesis rather than developmental lymphangiogenesis.

Sprouty4 KO mice are more resistant to ischemia

Next, we sought to investigate the effect of *Sprouty4* deficiency in the ischemia-induced angiogenesis model, an adult neovascularization assay which is useful for quantifying neovascularization in *Sprouty4* KO mice. We used mouse models of hind limb ischemia [23] and soft tissue ischemia [24]. We used *Sprouty4* KO mice, since *Sprouty4* KO mice can survive much longer than *Sprouty2* KO mice [21,25].

The former model revealed that *Sprouty4* KO mice were more resistant to hind limb ischemia than WT mice were (Fig. 3A). *Sprouty4* KO mice showed a significantly elevated recovery of limb perfusion after induction of hind limb ischemia as compared with WT mice, and the ischemic/non-ischemic leg perfusion ratio was much more favorable in *Sprouty4* KO mice than in WT mice ($P<0.001$) (Fig. 3B,C). Additionally, angiogenesis in the ischemic hind limb was significantly increased in *Sprouty4* KO mice compared with WT mice (Fig. 3D).

The latter model was induced by creating lateral skin incisions on the dorsal surfaces of mice. The overlying skin was undermined, and a silicone sheet was inserted into each mouse to separate the skin from the underlying tissue bed. As a result, the most central portion of skin underwent the most severe ischemic insult, which, in WT mice, ultimately led to the absence of flow and necrosis in the central portion of the skin (Fig. 4A). In *Sprouty4* KO mice, however, angiogenesis in the dorsal skin was significantly increased compared to that in WT mice (Fig. 4B). As a result, *Sprouty4* KO mice were more resistant to soft tissue ischemia than WT mice were, and gross evidence of necrosis in the dorsal skin was more evident in WT mice than in *Sprouty4* KO mice (100% and 16.7% in WT mice and *Sprouty4* KO mice, respectively, n = 6) (Fig. 4A).

These data show that *Sprouty4* KO mice exhibit enhanced neovascularization in ischemia-induced models.

Increased ischemia-induced neovascularization by *in vivo* shRNA targeting *Sproutys*

The increased vessel density in the skin and muscles of untreated *Sprouty4* KO mice (Fig. 2C,D, Fig. 3D) provides them with elevated blood-vessel area in these regions, which is partially responsible for their increased resistance to ischemia.

To investigate *in vivo* the efficiency of down-regulating *Sproutys* as therapy for peripheral ischemic diseases, we administered ischemia treatment to the hind limbs of C57BL/6J mice, then injected shRNA targeting *Sprouty2* and *Sprouty4*. We suppressed both *Sprouty2* and *Sprouty4* simultaneously, because both of the mRNAs increased during hind limb ischemia (Fig. 5A), because the phenotype of *Sprouty2*/*Sprouty4* DKO mice demonstrated a redundant role of *Sprouty2* and *Sprouty4* in angiogenesis (Fig. 1), and because we have not found any functional differences between Sprouty2 and Sprouty4 *in vitro* [20]. The shRNA plasmid targeting *Sprouty2* and *Sprouty4* efficiently suppressed the expression levels of endogenous Sprouty2 and Sprouty4, respectively, in both real-time PCR (Fig. 5B,C) and Western blot (Fig. 5D,E) analysis. The shRNA plasmids targeting both *Sprouty2* and *Sprouty4* enhanced VEGF-A-induced ERK and Akt activation *in vitro* in mouse embryonic fibroblasts (MEFs), which stably expressed VEGFR-2 (Fig. 5F). We used MEFs because it has been very difficult to introduce shRNA into primary murine endothelial cells *in vitro*. Although we confirmed that shRNA against Sprouty2 or Sprouty4 alone enhanced VEGF-A-induced ERK and Akt activation (data not shown), we observed much stronger effect by the combination of Sprouty2 and Sprouty4 shRNAs. Thus we decide to use combination of both Sprouty2 and Sprouty4 shRNAs for further experiments.

First, we showed that injection of shRNA plasmids targeting *Sprouty2* and *Sprouty4* significantly enhanced corneal neovascularization induced by VEGF-A, compared to control shRNA plasmids in a corneal micropocket assay (Fig. 6A–C). These data indicate that *Sprouty2* and *Sprouty4* shRNA plasmids can efficiently suppress the expression levels of Sprouty2 and Sprouty4 and block the effect of endogenous Sprouty2 and Sprouty4 *in vitro* and *in vivo*.

Next, we investigated whether *Sprouty2* and *Sprouty4* shRNA plasmids were effective in a mouse model of hind limb ischemia. Upon injection to the ischemic adductor muscle, *Sprouty2* and *Sprouty4* shRNA plasmids reduced *Sprouty2* and *Sprouty4* expression *in vivo* (Fig. 5A). *Sprouty2* and *Sprouty4* shRNA plasmids induced a significantly elevated recovery of limb perfusion after induction of hind limb ischemia as compared with control shRNA plasmids, and markedly improved the ischemic/non-ischemic leg perfusion ratio ($P<0.05$) (Fig. 7A,B). shRNA plasmids targeting *Sprouty2* and *Sprouty4* also increased capillary density compared with control shRNA plasmids (Fig. 7C). Our data clearly demonstrate that Sprouty2 and Sprouty4 negatively regulate angiogenesis *in vivo* and would make good therapeutic targets for peripheral ischemic diseases.

Discussion

In this study, we investigated the physiological function of Sproutys in angiogenesis by performing a knockout and knockdown analysis of *Sproutys*. In contrast to Spred1 and Spred2, which regulate developmental lymphangiogenesis, Sprouty2 and Sprouty4 are important negative regulators of developmental angiogenesis *in vivo*. We found that the amounts of blood vessels in *Sprouty4* KO mice are increased in all tissues we investigated. So we think that all peripheral blood vessels are increased in *Sprouty4* KO mice. *Sprouty4* deficiency enhanced ischemia-induced angiogenesis in mouse models of hind limb ischemia and soft tissue ischemia. Moreover, the suppression of *Sprouty2* and *Sprouty4* expression *in vivo* by shRNA targeting had a therapeutic effect in our model of hind limb ischemia, indicating that Sproutys should be novel therapeutic targets for treating peripheral ischemic diseases.

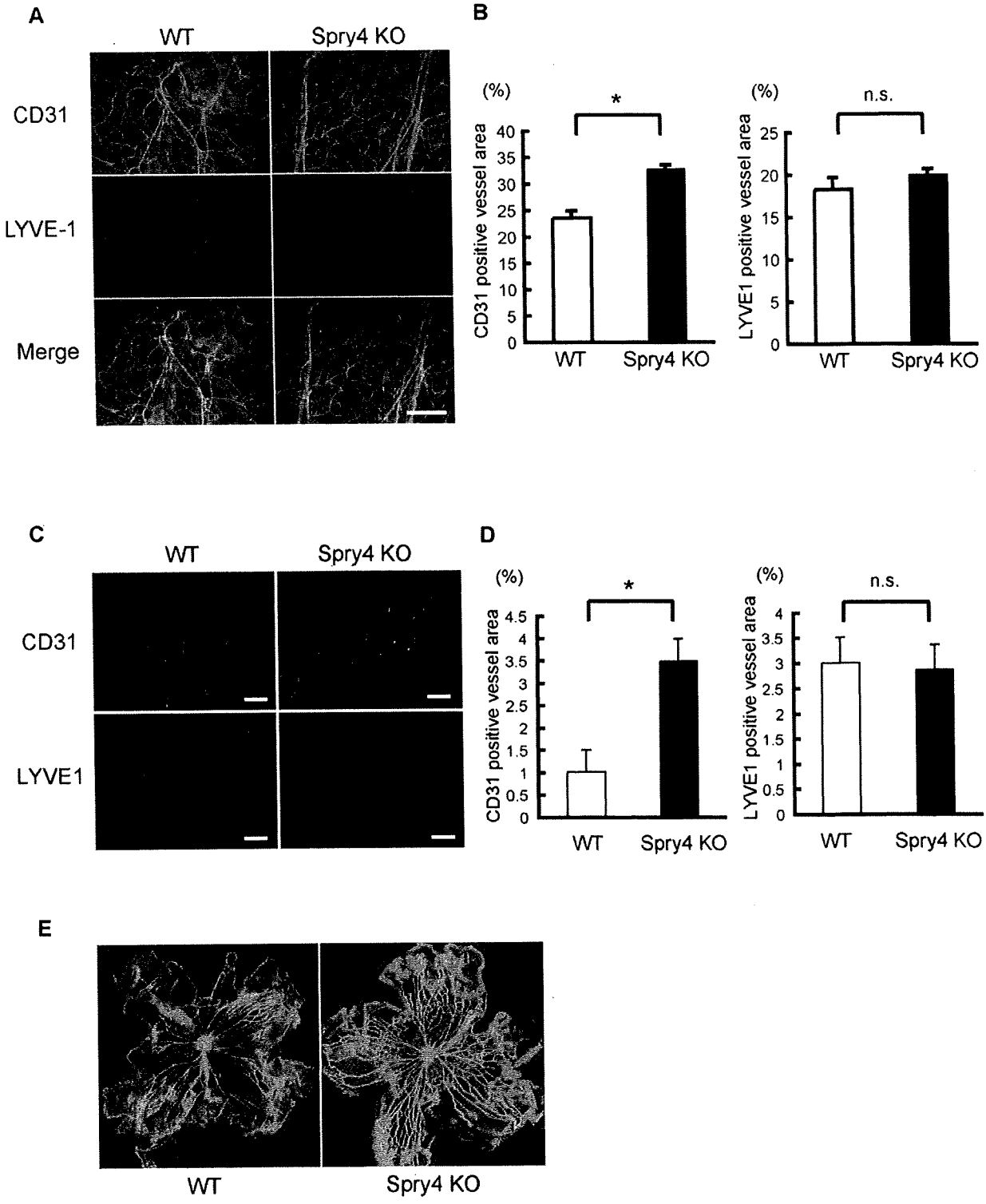

Figure 2. Blood and lymphatic vessels of *Sprouty4* single KO mice. (A) Blood vessels (green) and lymphatic vessels (red) in the ears of WT and *Sprouty4* KO mice (8 weeks old) were analyzed by whole-mount immunohistochemical staining with anti-PECAM-1/CD31Ab and anti-LYVE-1 Ab, respectively. (B) CD31-positive vessel area or LYVE1-positive area was quantified. Data shown are means±SEM. *: $P<0.05$. (C) Blood vessels (green) and lymphatic vessels (red) in the dorsal skin of WT and *Sprouty4* KO mice (8 weeks old) were analyzed by immunohistochemical staining with anti-PECAM-1/CD31Ab and anti-LYVE-1 Ab, respectively. Nuclei were stained with Hoechst 33342 dye (Blue). (D) CD31-positive vessel area or LYVE1-positive area was quantified. Data shown are means±SEM. *: $P<0.05$. (E) FITC-dextran-perfused flat-mounted retinal samples of WT and *Sprouty4* KO mice at postnatal day 3. Scale bars (A, C): 100 μm.
doi:10.1371/journal.pone.0005467.g002

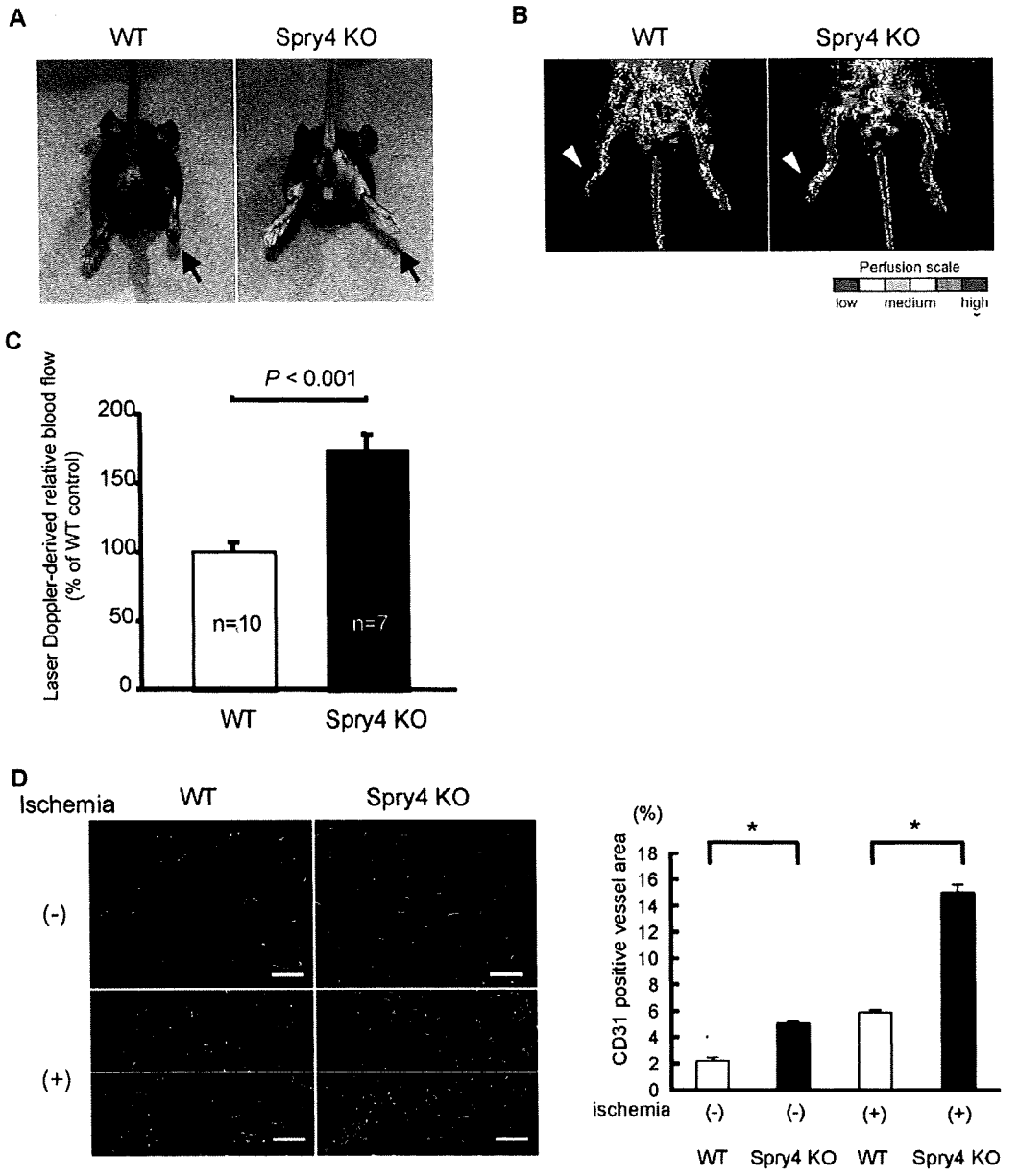

Figure 3. *Sprouty4* KO mice are more resistant in a hind-limb ischemia model. (A) Representative photos of ischemic limbs, indicated by arrows. (B) Representative laser Doppler images for each group are depicted. Arrowheads indicate ischemic limbs. The interval of low perfusion is displayed as dark blue; the highest perfusion interval is displayed as red. (C) Recovery of limb perfusion in WT (n = 10) and *Sprouty4* KO (n = 7) mice after hind limb ischemia as assessed by laser Doppler blood flow analysis on day 14. Data shown are means±SD. *: $P<0.001$. (D) Blood vessels (green) in the non-ischemic or ischemic adductor muscles of male WT and *Sprouty4* KO mice (8–10 weeks old) were analyzed by immunohistochemical staining with anti-PECAM-1/CD31Ab. Nuclei were stained with Hoechst 33342 dye (blue). The CD31-positive vessel area was quantified. Data shown are means±SEM. *: $P<0.05$. Scale bars: (D) 100 μm.
doi:10.1371/journal.pone.0005467.g003

The roles of Sprouty and Spred proteins during gastrulation in *Xenopus tropicalis* have been compared elsewhere [26]. Spred proteins preferentially inhibit the Ras/ERK cascade that directs mesoderm formation, whereas Sprouty proteins block the Ca^{2+} and PKCδ signals required for morphogenetic movements during gastrulation. Thus, the expression of *Sprouty* and *Spred* genes at specific times during gastrulation might redirect FGF signals toward mesoderm formation or morphogenesis, respectively [26].

In mammalian development, *Sproutys* are expressed mainly in blood endothelial cells, while *Spreds* are expressed mainly in lymphatic endothelial cells (Fig. 1G and Ref. [18]). In overexpression experiments, while Sproutys can inhibit VEGF-A signaling but not VEGF-C signaling, Spreds can suppress both types (Taniguchi K., unpublished data and Ref. [18]). Indeed, microRNA-126 deletion suppresses VEGF-A-induced ERK activation in endothelial cells and angiogenesis through the increase of

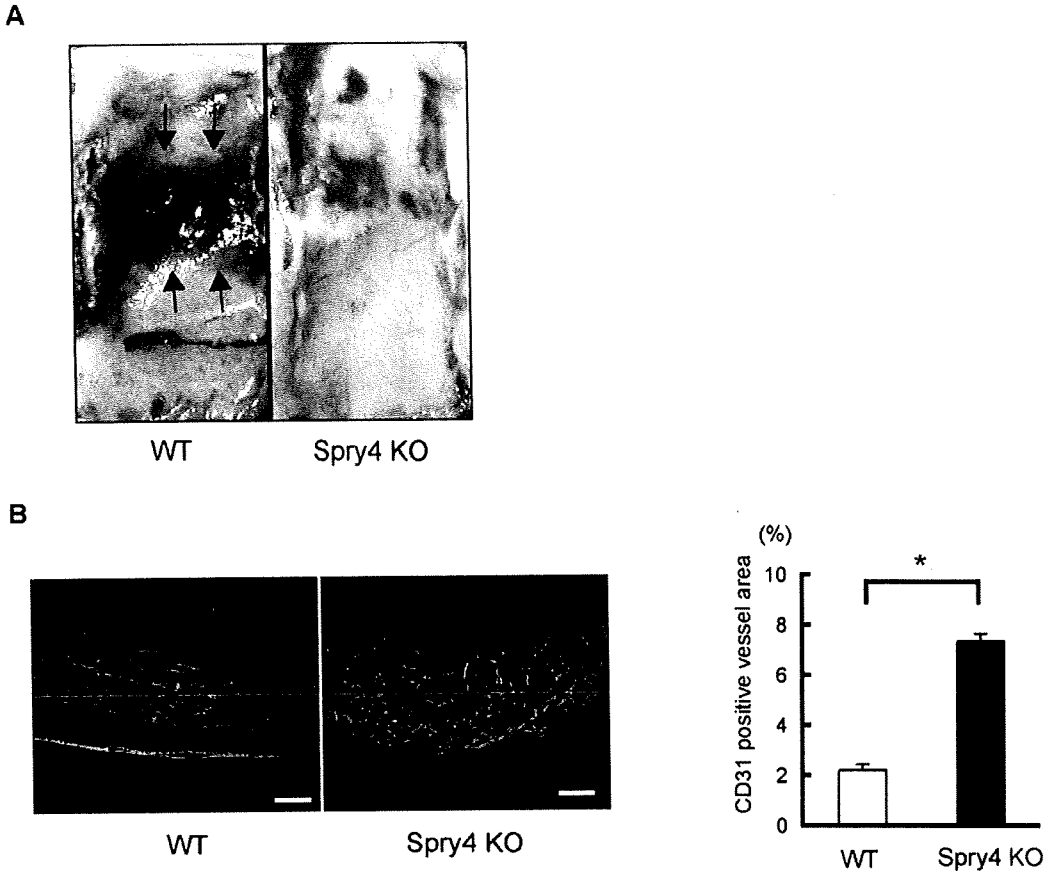

Figure 4. *Sprouty4* KO mice are also more resistant in a soft tissue ischemia model. (A) Representative photos of ischemic dorsal skin of male WT and *Sprouty4* KO mice (8–10 weeks old). Arrows indicate necrotic skin. (B) Left: Blood vessels (green) in the ischemic dorsal skin of male WT and *Sprouty4* KO mice were analyzed by immunohistochemical staining with anti-PECAM-1/CD31Ab. Nuclei were stained with Hoechst 33342 dye (blue). Right: The CD31-positive vessel area was quantified. Data shown are means±SEM. *: $P<0.05$. Scale bars (B): 100 μm.
doi:10.1371/journal.pone.0005467.g004

Spred1 [27–29]. However, the effect of *Sprouty* deletion is more specific to VEGF-A signaling than to VEGF-C signaling, while the effect of *Spred* deletion is more specific to VEGF-C signaling than to VEGF-A signaling (Taniguchi K., unpublished data and Ref. [18]). In fact, *Sprouty2* and *Sprouty4* single-deficient mice showed defects of blood vessels rather than lymphatic vessels, while *Spred1/Spred2* DKO mice showed abnormal lymphatic vessel development and nearly normal blood vessel development (Fig. 2 and Ref. [18]). In addition to this difference in expression, these results suggest that Sproutys and Spreds might have different functions in endothelial cells. VEGF-A/VEGFR-2 signaling is Ras-independent and PLC-γ/PKC-dependent, while VEGF-C/VEGFR-3 signaling is Ras-dependent and PKC-independent (Taniguchi K., unpublished data and Ref. [4]). Therefore, drawing an analogy from the different functions of Sproutys and Spreds in *Xenopus tropicalis*, we propose that Sproutys inhibit PLC-γ/PKC-dependent VEGF-A signaling and angiogenesis, while Spreds inhibit Ras-dependent VEGF-C signaling and lymphangiogenesis.

Although, in ischemia-induced angiogenesis, VEGF-A is thought to be the primary angiogenesis-stimulating factor [30], angiogenesis is the more complex process, as it is triggered not only by VEGF-A but also by bFGF, S1P, angiopoietins, and others [12–14]. In fact, it is reported that *bFGF* gene therapy is effective to treat critically ischemic limb [31]. It is already known that Sproutys can inhibit various RTK signals [1,2]. We have also shown that loss of *Sprouty* expression results in hyperactivation of VEGF-A and bFGF signaling as well as S1P and LPA signaling (Fig. 5F, Taniguchi K., unpublished data and Ref. [19] and [21]). It is reported that *in vivo* shRNA targeting *SHP-1* also accelerated angiogenesis in a rat model of hind limb ischemia [32]. While SHP-1 inhibits only RTK signals, Sproutys suppress both RTK and GPCR signals. Thus the suppression of *Sproutys* could be beneficial.

Inhibition of negative feed-back loops leading to profound and long term activation of signals often lead to a dysregulation of neovascularisation since the overshooting response is inducing immature vessels. However, excessive sprouting in response to inhibition of Sproutys results in the formation of mature vessels. Angiogenesis is a complex process that includes the recruitment and proliferation of various cells, such as endothelial cells, mural cells [smooth muscle cells (SMC) and pericytes], endothelial progenitor cells (EPCs) and others. It is reported that *Sprouty*-family genes are expressed in both endothelial cells and smooth muscle cells [33], and we have confirmed that *Sprouty/Spred* family genes are also expressed in bone marrow (Taniguchi K., unpublished data). It is possible that Sproutys function not only in endothelial cells, but also in mural cells, EPCs or myeloid cells, and that enhanced angiogenesis of mature vessels in *Sprouty4* KO mice and

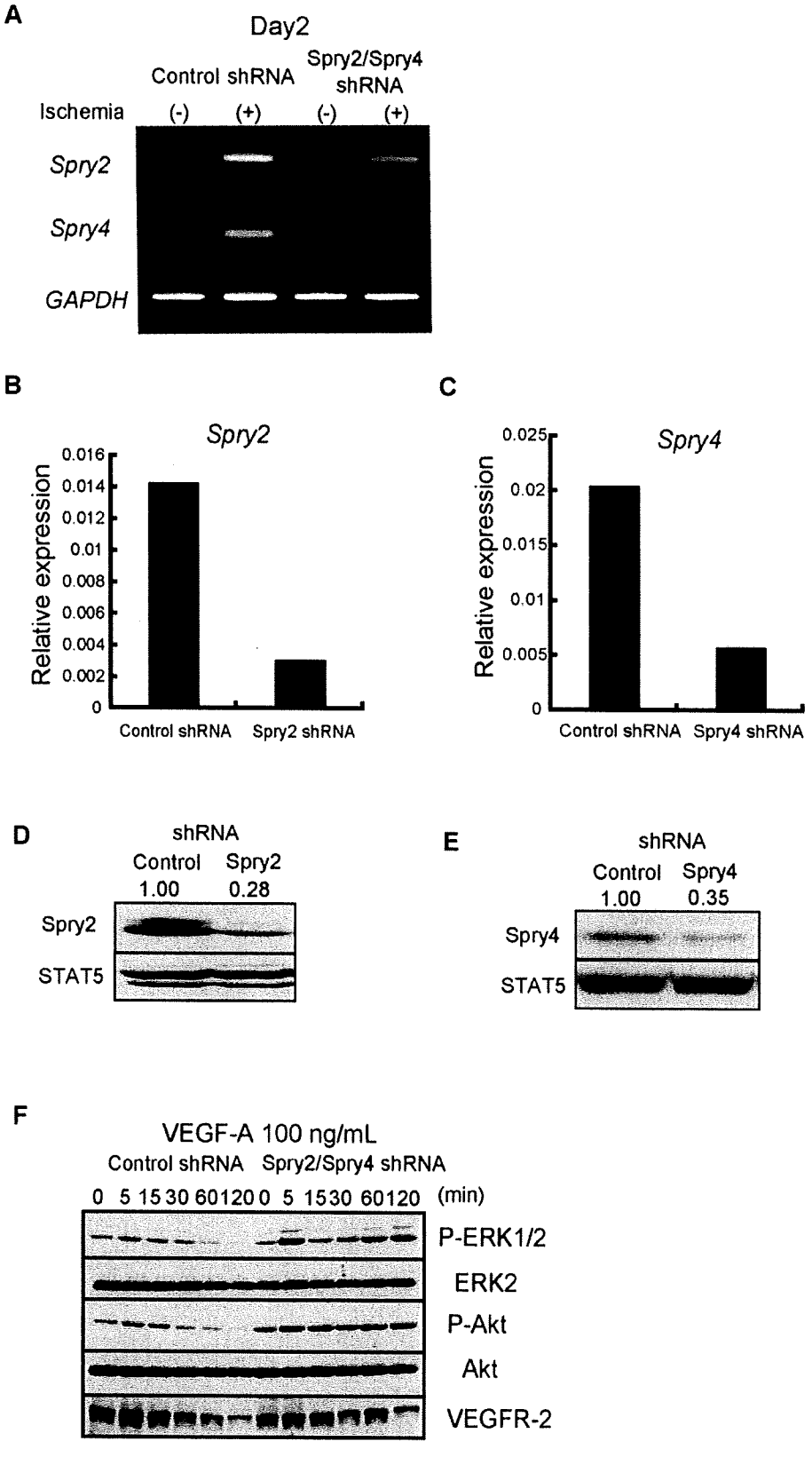
A
Day2
Control shRNA
Spry2/Spry4 shRNA
Ischemia
(-) (+) (-) (+)
Spry2
Spry4
GAPDH
B
Spry2
Relative expression
0.016
0.014
0.012
0.01
0.008
0.006
0.004
0.002
0
Control shRNA
Spry2 shRNA
C
Spry4
Relative expression
0.025
0.02
0.015
0.01
0.005
0
Control shRNA
Spry4 shRNA
D
shRNA
Control
Spry2
1.00
0.28
Spry2
STAT5
E
shRNA
Control
Spry4
1.00
0.35
Spry4
STAT5
F
VEGF-A 100 ng/mL
Control shRNA
Spry2/Spry4 shRNA
0 5 15 30 60 120 0 5 15 30 60 120 (min)
P-ERK1/2
ERK2
P-Akt
Akt
VEGFR-2

Figure 5. *In vivo* effects of shRNA targeting *Sprouty2* and *Sprouty4*. (A) The *in vivo* effects of shRNA plasmids targeting *Sproutys* in the hind limb model were evaluated by RT-PCR analysis. (B, C) Real-time PCR analysis of *Sprouty2* (B) or *Sprouty4* (C) mRNA expression in MEFs stably infected with control retroviruses and retroviruses expressing either *Sprouty2* shRNA (B) or *Sprouty4* shRNA (C). (D, E) Western blot analysis of protein extracts from MEFs stably infected with control retroviruses and retroviruses expressing either *Sprouty2* shRNA (D) or *Sprouty4* shRNA (E). The relative intensities of Sprouty2 and Sprouty4 bands normalized by STAT5 expression levels are shown above. (F) Effect of both *Sprouty2* and *Sprouty4* knockdown on ERK and Akt activities. MEFs stably expressing VEGFR-2 were infected with control retroviruses and retroviruses expressing *Sprouty2*/*Sprouty4* shRNA, and stimulated with 100 ng/mL VEGF-A. Cell extracts were immunoblotted with the indicated antibodies.
doi:10.1371/journal.pone.0005467.g005

the results of our experiments with *in vivo* shRNA targeting *Sproutys* are partially dependent on the enhanced function or the increased number of mural cells, EPCs or myeloid cells. Moreover, it is possible that Sproutys are also associated with angiopoietins signals, which are important for the maturation of blood vessels. Further study is necessary to investigate these possibilities.

Sprouty4 KO mice were more resistant to ischemia than WT mice were in mouse models of ischemia (Fig. 3, Fig. 4), and neovascularization induced by a tumor transplantation model was also accelerated by *Sprouty4* deficiency (Taniguchi K., unpublished data). Moreover, *in vivo* shRNA targeting *Sprouty2* and *Sprouty4* accelerated angiogenesis in a mouse model of hind limb ischemia (Fig. 7). In this study, muscle tissue injected with the *Sproutys* shRNA vectors exhibited a significant decrease in *Sproutys* transcripts (Fig. 5A). This knockdown efficiency may be due to the fact, in skeletal muscle, the efficiency of intramuscular gene transfer has been shown to be augmented from five- to seven-fold when the injected muscle is ischemic [34]. The present study is the first to uncover these significant implications for gene therapy using the *Sprouty2* and *Sprouty4* shRNA vectors for the treatment of peripheral ischemic diseases. The fact that Sproutys exhibit such broad suppression activity, inhibiting a wide variety of angiogenic factors and cells, indicates that the suppression of *Sproutys* must enhance neovascularization.

In conclusion, Sproutys are physiologically important regulators of angiogenesis *in vivo* and may be useful as new therapeutic targets for peripheral ischemic diseases.

Methods

Mice

Sprouty2 KO mice and *Sprouty4* KO mice have been described previously [21,25]. *Sprouty2* KO mice and *Sprouty4* KO mice were generated as 129/C57BL/6J mixed background, and then backcrossed into C57BL/6J at least five times. Gender-matched, WT littermates were used as controls. All experiments using these mice were approved by and performed according to the guidelines of the Animal Ethics Committee of Kyushu University, Fukuoka, Japan.

Cell culture

Primary mouse embryonic fibroblasts (MEFs) were prepared, as previously described [21]. MEFs were cultured in Dulbecco's modified Eagle's medium (DMEM) (Gibco, Grand Island, NY, USA) supplemented with 10% fetal bovine serum, penicillin and streptomycin. To generate MEFs stably expressing VEGFR-2 or shRNAs, MEFs were infected with the retroviruses produced by

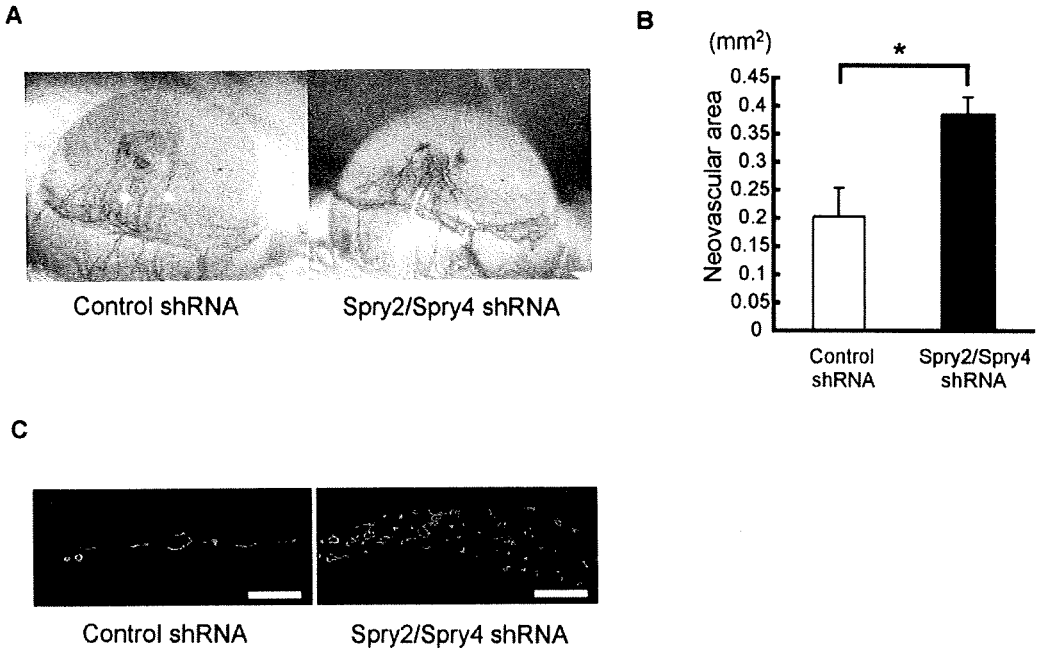

Figure 6. *In vivo* effects of shRNA targeting *Sprouty2* and *Sprouty4* in corneal micropocket assay. (A) Corneal neovascularization was induced by mouse VEGF-A (200 ng) on day 12 after hydron pellets had been implanted into male BALB/c mouse corneas. After implantation, 10 μg shRNA plasmids per eye were delivered by subconjunctival injection. Representative photos are shown. (B) Quantitative analysis of neovascularization on day 12. Areas are expressed in mm^2. Bars show the mean±SEM (n = 5). *: $P<0.05$. (C) Sections of corneas implanted with VEGF-A stained by anti-PECAM-1/CD31Ab on day 12. Scale bars (C): 100 μm.
doi:10.1371/journal.pone.0005467.g006

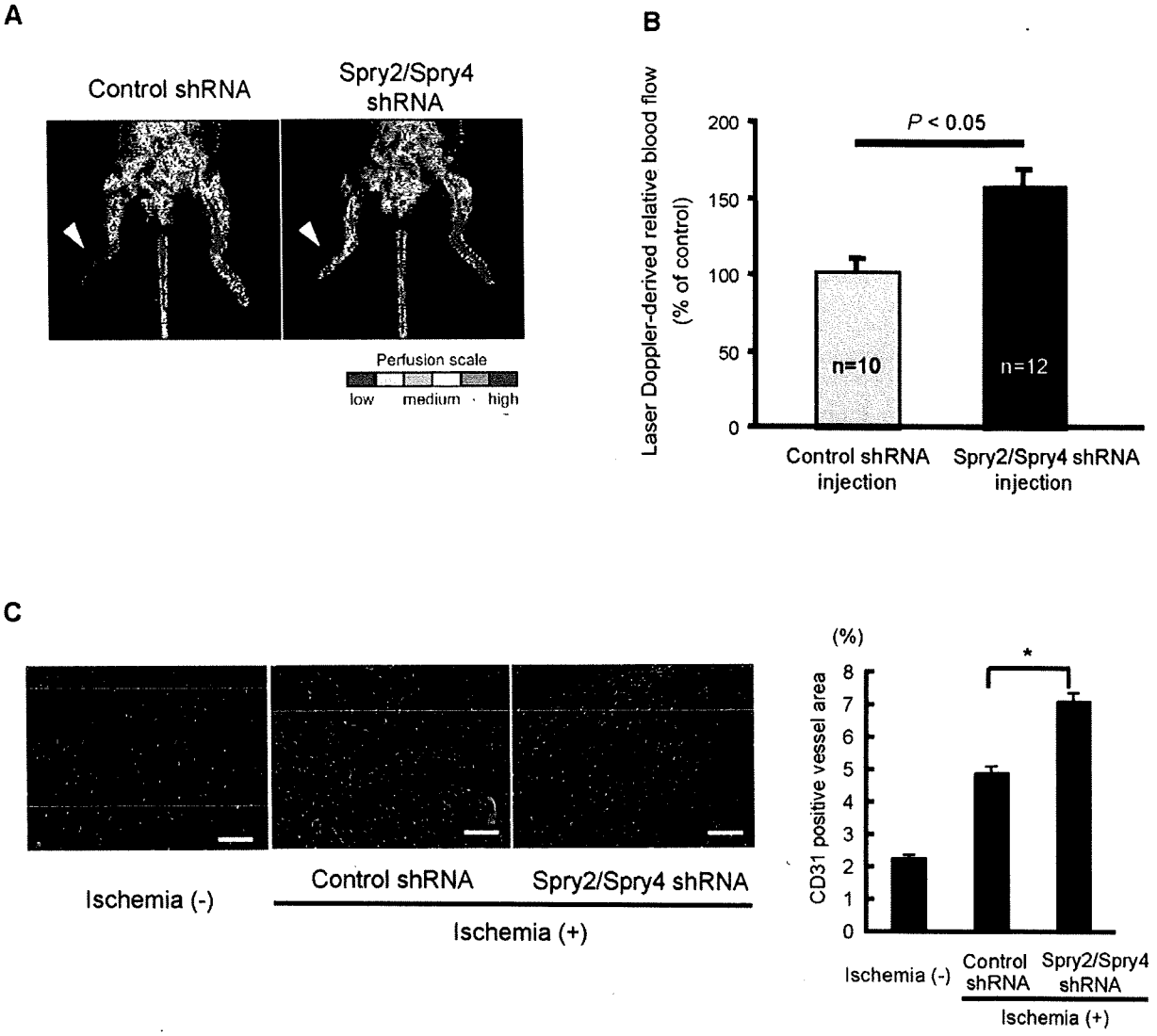

Figure 7. Increased ischemia-induced angiogenesis by *in vivo* shRNA targeting *Sprouty2 and Sprouty4*. (A) Representative laser Doppler images for each group are depicted. Arrowheads indicate ischemic limbs. The interval of low perfusion is displayed as dark blue; the highest perfusion interval is displayed as red. (B) Recovery of limb perfusion in C57BL/6J mice (8 weeks old) injected with the control shRNA (n = 10) or *Sprouty2/Sprouty4* shRNA vectors (n = 12) after hind limb ischemia as assessed by laser Doppler blood flow analysis on day 14. Data shown are means±SD. *: $P<0.05$. (C) Blood vessels (green) in the non-ischemic or ischemic adductor muscle injected with the control shRNA or *Sprouty2/Sprouty4* shRNA vectors stained with anti-PECAM-1/CD31Ab. Nuclei were stained with Hoechst 33342 dye (blue). The CD31-positive vessel area was quantified. Data shown are means±SEM. *: $P<0.05$. Scale bars (C): 100 μm.
doi:10.1371/journal.pone.0005467.g007

Plat-E, packaging cell line, transfected with pMX-VEGFR-2 or shRNA plasmids, and then the infected cells were selected with 1 μg/ml puromycin (Invivogen, San Diego, CA, USA), as previously described [18,35].

Antibodies and reagents

Antibodies used in this experiment were as follows: anti-phospho-ERK1/2 (#9106), anti-phospho-Akt (#4058), and anti-Akt (#9272) (Cell Signaling Technology, Danvers, MA, USA); anti-Sprouty4 (H-100), anti-VEGFR-2 (A-3) and anti-ERK2 (C-14) (Santa Cruz Biotechnology, Santa Cruz, CA, USA); anti-Sprouty2 (ab50317) (Abcam, Cambridge, MA, USA); and anti-vWF (DAKO, Glostrup, Denmark); Mouse VEGF-A was purchased from R&D Systems (Minneapolis, MN, USA). Human VEGF-A was purchased from PeproTech (London, UK).

RT-PCR and real-time PCR analysis

The cells or tissues were lysed in RNAiso (TAKARA BIO, Shiga, Japan) for RNA preparation. Total RNA was isolated through fluorescence activated cell sorting (FACS), which sorted about 5.0×10^4 BECs and LECs at embryonic day 14.5, as previously reported [18]. Good separation of BECs and LECs was confirmed by BEC markers (*Nrp1*, *CD44*) and LEC markers (*LYVE-1*, *Prox1*). Total RNA was reverse transcribed using the High Capacity cDNA Reverse Transcription Kit (Applied Biosystems, Foster City, CA, USA), and the product was used

for further analysis. PCR products were separated on 2.0% agarose gel stained with ethidium bromide. The expression level of *GAPDH* was evaluated as an internal control. The primer sequences for RT-PCR were as follows: *Sprouty2*-F, 5′- TTTTAATCCACCGATTGCTTGG-3′; *Sprouty2*-R, 5′-GCTGCACTCGGATTATTCCATC-3′; *Sprouty4*-F, 5′-CAGCTCCTCAAAGACCCCTAGAAGC-3′; *Sprouty4*-R, 5′-GTGCTGCTACTGCTGCTTACAGAGC-3′; *GAPDH*-F, 5′-ACCACAGTCCATGCCATCAC-3′ and *GAPDH*-R 5′-TCCACCACCCTGTTGCTGTA-3′. The primer sequences for BEC and LEC markers were described elsewhere [36]. Real-time PCR was performed on cDNA samples using an ABI 7000 Sequence Detection System (Applied Biosystems) with the SYBR Green system (Applied Biosystems). The relative quantitation value is expressed as 2^{-Ct}, where *Ct* is the difference between the mean *Ct* value of triplicates of the sample and of the endogenous *GAPDH* control. The primer sequences for real-time PCR were as follows: *Sprouty2*-F, 5′-ATAATCCGAGTGCAGCCTAAATC-3′; *Sprouty2*-R, 5′-CGCAGTCCTCACACCTGTAG-3′; *Sprouty4*-F, 5′-CGACCAGAGGCTCCTAGATCA-3′; *Sprouty4*-R, 5′-CAGCGGCTTACAGTGAACCA-3′; *GAPDH*-F, 5′-TGTGTCCGTCGTGGATCTGA-3′ and *GAPDH*-R 5′-CCTGCTTCACCACCTTCTTGA-3′.

Western blot analysis

Western blot analysis was performed as described previously [18]. MEFs were lysed in lysis buffer (50 mM Tris-HCl, pH 7.6, 150 mM NaCl, 1% Nonidet P-40, 1 mM sodium vanadate) supplemented with protease inhibitors (Nacalai tesque, Kyoto, Japan). About 20 μg of proteins were separated by SDS-PAGE and transferred to Immobilon-P nylon membranes (Millipore, Bedford, MA, USA).

Immunohistochemistry

Whole-mount immunohistochemistry of adult ears or immunohistochemistry of adult skin was performed with 1:200 diluted anti-PECAM-1/CD31 (MEC13.3, BD Pharmingen, Franklin Lakes, NJ, USA) or anti-LYVE-1 antibody (Acris Antibodies, Hiddenhausen, Germany) essentially as described previously [18].

Retinal angiography

Flat-mounted retinas were evaluated using fluorescein–dextran angiography as described elsewhere [22]. The mice were deeply anesthetized and a 0.03 ml/g body weight 50 mg/mL solution of 2×10^6 molecular weight FITC–dextran (Sigma, St Louis, MO, USA) was perfused through the left ventricle. The eyes were enucleated and fixed in 4% paraformaldehyde for at least 3 h. The corneas and lenses were then removed, and the peripheral retinas were dissected and flat-mounted on microscope slides for examination under a fluorescence microscope.

Vessel quantitative analysis

The vascular area in the ear, skin or muscle was quantified as a PECAM-1/CD31-positive area from ten ×10 micrographs, using Image J software (http://rsb.info.nih.gov), as described elsewhere [37]. LYVE-1-positive vessels in the skin were quantified in a similar manner.

RNAi-mediated knockdown

The mammalian expression vector pSUPER.retro.puro (Oligoengine, Seattle, WA, USA) was used for expression of shRNA targeting murine *Sprouty2*. The sequence of the *Sprouty2* shRNA is 5′-GCCGGGTTGTCGTTGTAAA-3′ and corresponds to nucleotides 1150–1168 of *mSprouty2*. Murine *Sprouty4* shRNA (29-mer) and control plasmids were purchased from Origene (Rockville, MD, USA) and used according to the manufacturer's protocols. The specificity of *Sprouty2* and *Sprouty4* knockdown was confirmed by real-time PCR or immunoblotting of whole-cell lysates of MEFs with anti-Sprouty2 and anti-Sprouty4 antibodies, respectively. The relative intensities of Sprouty2 or Sprouty4 band were normalized by STAT5 expression using Image J software, as previously described [9,35].

In vivo models of ischemia

A hind limb ischemia model was performed as previously described [23,38]. Male WT and *Sprouty4* KO mice (8–10 weeks old) and male C57BL/6J mice (8 weeks old) were used for a hind limb ischemia model. The proximal portion of the right femoral artery including the superficial and the deep branch and the distal portion of the saphenous artery were occluded with an electrical coagulator. After 2 weeks, we determined the ischemic (right)/nonischemic (left) limb blood flow ratio by using a laser Doppler blood flow imager (Laser Doppler Perfusion Imager System, moorLDI-Mark 2; Moor Instruments, Wilmington, DE, USA). Before initiating scanning, mice were placed on a heating pad at 37°C to minimize variations in their body temperatures. Calculated perfusion is expressed as the ratio of ischemic to nonischemic hind limb perfusion. At 2 wk after femoral resection, adductor muscles from the ischemic and control limbs were embedded in OCT compound. Eight-micron sections were stained with anti-PECAM-1/CD31 antibody (BD Pharmingen) and anti-rat Ig secondary antibody. For *in vivo* shRNA targeting *Sprouty2* and *Sprouty4*, a hind limb ischemia model was performed. Immediately after ischemia was induced, either a total of 40 μg *Sproutys* shRNA vectors (20 μg *Sprouty2* shRNA vector and 20 μg *Sprouty4* shRNA vector) or a quantity of control shRNA vectors was injected into five different sites in the adductor muscle of each anesthetized mouse [32]. A model of soft tissue ischemia similar to one described elsewhere [24,39] was developed. The model consisted of lateral skin incisions (2.5 cm in length and 1.25 cm apart) created on the dorsal surface of mice, penetrating the skin, dermis, and underlying adipose tissue. The overlying skin was undermined, and a 0.13-mm-thick silicone sheet was inserted to separate the skin from the underlying tissue bed. The skin was then reapproximated with 6-0 nylon sutures.

Corneal micropocket assay

The mouse corneal micropocket assay and quantification of neovascularization were performed as described elsewhere [40], using male BALB/c mice (6–10 weeks old). For local delivery, shRNA plasmids (total 10 μg/10 μl per eye) were diluted in phosphate-buffered saline (PBS) and delivered subconjunctivally. The subconjunctival injections were given after hydron pellet implantation.

Statistical analysis

Data are expressed as mean±SD or mean±SEM. Statistical significance was tested with an unpaired two-tailed Student's *t*-test or analysis of variance (ANOVA). The differences were considered to be significant if $P<0.05$.

Acknowledgments

We thank T. Yoshioka, K. Fukuse, M. Asakawa, N. Shiino, H. Fujii, N. Kinoshita, M. Ohtsu, and Y. Yamada for technical assistance, and Y. Nishi and N. Soma for manuscript preparation. We also thank Dr. H. Nishinakamura for technical advice.

Author Contributions

Conceived and designed the experiments: KT HY TI HK YS MO YY AY. Performed the experiments: KT KiS KW TA FO RiK. Analyzed the data: KT KiS KW RiK. Contributed reagents/materials/analysis tools: KT TI RK. Wrote the paper: KT AY.

References

1. Kim HJ, Bar-Sagi D (2004) Modulation of signalling by Sprouty: a developing story. Nat Rev Mol Cell Biol 5: 441–450.
2. Mason JM, Morrison DJ, Basson MA, Licht JD (2006) Sprouty proteins: multifaceted negative-feedback regulators of receptor tyrosine kinase signaling. Trends Cell Biol 16: 45–54.
3. Cabrita MA, Christofori G (2008) Sprouty proteins, masterminds of receptor tyrosine kinase signaling. Angiogenesis 11: 53–62.
4. Takahashi T, Yamaguchi S, Chida K, Shibuya M (2001) A single autophosphorylation site on KDR/Flk-1 is essential for VEGF-A-dependent activation of PLC-gamma and DNA synthesis in vascular endothelial cells. Embo J 20: 2768–2778.
5. Hacohen N, Kramer S, Sutherland D, Hiromi Y, Krasnow MA (1998) sprouty encodes a novel antagonist of FGF signaling that patterns apical branching of the Drosophila airways. Cell 92: 253–263.
6. Casci T, Vinos J, Freeman M (1999) Sprouty, an intracellular inhibitor of Ras signaling. Cell 96: 655–665.
7. Wakioka T, Sasaki A, Kato R, Shouda T, Matsumoto A, et al. (2001) Spred is a Sprouty-related suppressor of Ras signalling. Nature 412: 647–651.
8. Kato R, Nonami A, Taketomi T, Wakioka T, Kuroiwa A, et al. (2003) Molecular cloning of mammalian Spred-3 which suppresses tyrosine kinase-mediated Erk activation. Biochem Biophys Res Commun 302: 767–772.
9. Brems H, Chmara M, Sahbatou M, Denayer E, Taniguchi K, et al. (2007) Germline loss-of-function mutations in SPRED1 cause a neurofibromatosis 1-like phenotype. Nat Genet 39: 1120–1126.
10. Flamme I, Frolich T, Risau W (1997) Molecular mechanisms of vasculogenesis and embryonic angiogenesis. J Cell Physiol 173: 206–210.
11. Folkman J (1995) Angiogenesis in cancer, vascular, rheumatoid and other disease. Nat Med 1: 27–31.
12. Hanahan D (1997) Signaling vascular morphogenesis and maintenance. Science 277: 48–50.
13. Shibuya M (2008) Vascular endothelial growth factor-dependent and -independent regulation of angiogenesis. BMB Rep 41: 278–286.
14. Hannun YA, Obeid LM (2008) Principles of bioactive lipid signalling: lessons from sphingolipids. Nat Rev Mol Cell Biol 9: 139–150.
15. Impagnatiello MA, Weitzer S, Gannon G, Compagni A, Cotten M, et al. (2001) Mammalian sprouty-1 and -2 are membrane-anchored phosphoprotein inhibitors of growth factor signaling in endothelial cells. J Cell Biol 152: 1087–1098.
16. Lee SH, Schloss DJ, Jarvis L, Krasnow MA, Swain JL (2001) Inhibition of angiogenesis by a mouse sprouty protein. J Biol Chem 276: 4128–4133.
17. Sasaki A, Taketomi T, Kato R, Saeki K, Nonami A, et al. (2003) Mammalian Sprouty4 suppresses Ras-independent ERK activation by binding to Raf1. Nat Cell Biol 5: 427–432.
18. Taniguchi K, Kohno R, Ayada T, Kato R, Ichiyama K, et al. (2007) Spreds are essential for embryonic lymphangiogenesis by regulating vascular endothelial growth factor receptor 3 signaling. Mol Cell Biol 27: 4541–4550.
19. Ayada T, Taniguchi K, Okamoto F, Kato R, Komune S, et al. (2009) Sprouty4 negatively regulates protein kinase C activation by inhibiting phosphatidylinositol 4,5-biphosphate hydrolysis. Oncogene 28: 1076–1088.
20. Sasaki A, Taketomi T, Wakioka T, Kato R, Yoshimura A (2001) Identification of a dominant negative mutant of Sprouty that potentiates fibroblast growth factor- but not epidermal growth factor-induced ERK activation. J Biol Chem 276: 36804–36808.
21. Taniguchi K, Ayada T, Ichiyama K, Kohno R, Yonemitsu Y, et al. (2007) Sprouty2 and Sprouty4 are essential for embryonic morphogenesis and regulation of FGF signaling. Biochem Biophys Res Commun 352: 896–902.
22. D'Amato R, Wesolowski E, Smith LE (1993) Microscopic visualization of the retina by angiography with high-molecular-weight fluorescein-labeled dextrans in the mouse. Microvasc Res 46: 135–142.
23. Sasaki K, Heeschen C, Aicher A, Ziebart T, Honold J, et al. (2006) Ex vivo pretreatment of bone marrow mononuclear cells with endothelial NO synthase enhancer AVE9488 enhances their functional activity for cell therapy. Proc Natl Acad Sci U S A 103: 14537–14541.
24. Tepper OM, Capla JM, Galiano RD, Ceradini DJ, Callaghan MJ, et al. (2005) Adult vasculogenesis occurs through in situ recruitment, proliferation, and tubulization of circulating bone marrow-derived cells. Blood 105: 1068–1077.
25. Taketomi T, Yoshiga D, Taniguchi K, Kobayashi T, Nonami A, et al. (2005) Loss of mammalian Sprouty2 leads to enteric neuronal hyperplasia and esophageal achalasia. Nat Neurosci 8: 855–857.
26. Sivak JM, Petersen LF, Amaya E (2005) FGF signal interpretation is directed by Sprouty and Spred proteins during mesoderm formation. Dev Cell 8: 689–701.
27. Wang S, Aurora AB, Johnson BA, Qi X, McAnally J, et al. (2008) The endothelial-specific microRNA miR-126 governs vascular integrity and angiogenesis. Dev Cell 15: 261–271.
28. Fish JE, Santoro MM, Morton SU, Yu S, Yeh RF, et al. (2008) miR-126 regulates angiogenic signaling and vascular integrity. Dev Cell 15: 272–284.
29. Kuhnert F, Mancuso MR, Hampton J, Stankunas K, Asano T, et al. (2008) Attribution of vascular phenotypes of the murine Egfl7 locus to the microRNA miR-126. Development 135: 3989–3993.
30. Schalch P, Patejunas G, Retuerto M, Sarateanu S, Milbrandt J, et al. (2004) Homozygous deletion of early growth response 1 gene and critical limb ischemia after vascular ligation in mice: evidence for a central role in vascular homeostasis. J Thorac Cardiovasc Surg 128: 595–601.
31. Masaki I, Yonemitsu Y, Yamashita A, Sata S, Tanii M, et al. (2002) Angiogenic gene therapy for experimental critical limb ischemia: acceleration of limb loss by overexpression of vascular endothelial growth factor 165 but not of fibroblast growth factor-2. Circ Res 90: 966–973.
32. Sugano M, Tsuchida K, Maeda T, Makino N (2007) SiRNA targeting SHP-1 accelerates angiogenesis in a rat model of hindlimb ischemia. Atherosclerosis 191: 33–39.
33. Antoine M, Wirz W, Tag CG, Mavituna M, Emans N, et al. (2005) Expression pattern of fibroblast growth factors (FGFs), their receptors and antagonists in primary endothelial cells and vascular smooth muscle cells. Growth Factors 23: 87–95.
34. Takeshita S, Isshiki T, Sato T (1996) Increased expression of direct gene transfer into skeletal muscles observed after acute ischemic injury in rats. Lab Invest 74: 1061–1065.
35. Nishinakamura H, Minoda Y, Saeki K, Koga K, Takaesu G, et al. (2007) An RNA-binding protein alphaCP-1 is involved in the STAT3-mediated suppression of NF-kappaB transcriptional activity. Int Immunol 19: 609–619.
36. Morisada T, Oike Y, Yamada Y, Urano T, Akao M, et al. (2005) Angiopoietin-1 promotes LYVE-1-positive lymphatic vessel formation. Blood 105: 4649–4656.
37. Tammela T, Zarkada G, Wallgard E, Murtomaki A, Suchting S, et al. (2008) Blocking VEGFR-3 suppresses angiogenic sprouting and vascular network formation. Nature 454: 656–660.
38. Chavakis E, Aicher A, Heeschen C, Sasaki K, Kaiser R, et al. (2005) Role of beta2-integrins for homing and neovascularization capacity of endothelial progenitor cells. J Exp Med 201: 63–72.
39. Kimura H, Miyashita H, Suzuki Y, Kobayashi M, Watanabe K, et al. (2009) Distinctive localization and opposed roles of vasohibin-1 and vasohibin-2 in the regulation of angiogenesis. Blood, in press.
40. Nakao S, Kuwano T, Tsutsumi-Miyahara C, Ueda S, Kimura YN, et al. (2005) Infiltration of COX-2-expressing macrophages is a prerequisite for IL-1 beta-induced neovascularization and tumor growth. J Clin Invest 115: 2979–2991.

The American Journal of Pathology, Vol. 175, No. 1, July 2009
Copyright © American Society for Investigative Pathology
DOI: 10.2353/ajpath.2009.080788

Vascular Biology, Atherosclerosis and Endothelium Biology

Vasohibin-1 Expression in Endothelium of Tumor Blood Vessels Regulates Angiogenesis

Tomoko Hosaka,*† Hiroshi Kimura,* Takahiro Heishi,* Yasuhiro Suzuki,* Hiroki Miyashita,* Hideki Ohta,‡ Hikaru Sonoda,‡ Takuya Moriya,§ Satoshi Suzuki,† Takashi Kondo,† and Yasufumi Sato*

From the Departments of Vascular Biology, and Thoracic Surgery,† Institute of Development, Aging and Cancer, Tohoku University, Sendai; the Discovery Research Laboratories,‡ Shionogi & Co. Ltd, Osaka; and the Department of Pathology,§ Tohoku University Hospital, Sendai, Japan*

In this study, we characterized the significance of the vascular endothelial growth factor-inducible angiogenesis inhibitor vasohibin-1 to tumors. In pathological sections of non-small cell lung carcinoma, vasohibin-1 was present in the endothelial cells of blood vessels of the tumor stroma, but not in the lymphatics. In cancer cells, the presence of vasohibin-1 was associated with hypoxia-inducible factor 1α/vascular endothelial growth factor and fibroblast growth factor-2 expression. We then examined the function of vasohibin-1 in the mouse by subcutaneously inoculating with Lewis lung carcinoma cells. Resultant tumors in *vasohibin-1*$^{-/-}$ mice contained more immature blood vessels and fewer apoptotic tumor cells than tumors in wild-type mice. In wild-type mice that had been inoculated with Lewis lung carcinoma cells, tail vein injection of adenovirus containing the human *vasohibin-1* gene inhibited tumor growth and tumor angiogenesis. Moreover, the remaining tumor vessels in adenoviral human *vasohibin-1* gene-treated mice were small, round, and mature, surrounded by mural cells. The addition of adenoviral human *vasohibin-1* gene to cisplatin treatment improved cisplatin's antitumor activity in mice. These results suggest that endogenous vasohibin-1 is not only involved in tumor angiogenesis, but when sufficient exogenous vasohibin-1 is supplied, it blocks sprouting angiogenesis by tumors, matures the remaining vessels, and enhances the antitumor effect of conventional chemotherapy. *(Am J Pathol 2009, 175:430–439; DOI: 10.2353/ajpath.2009.080788)*

Angiogenesis, also called neovascularization, is a fundamental process of blood vessel growth, and a hallmark of cancer development. Multiple studies show that tumor angiogenesis in non-small cell lung carcinoma (NSCLC) is associated with metastases and poor survival.[1] The importance of tumor angiogenesis is further emphasized by clinical studies of anti-angiogenic agents.[2] Indeed, anti-angiogenic therapy shows promise as an effective treatment for various cancers, including NSCLC.[3]

The local balance between angiogenesis stimulators and inhibitors regulates angiogenesis. The most important molecule that stimulates angiogenesis is vascular endothelial growth factor (VEGF).[4] The circulating level of VEGF before treatment predicts the survival of patients with NSCLC.[5–7] Hypoxia, one of the triggers of angiogenesis, induces the expression of various molecules including VEGF. Hypoxia frequently occurs in tumors due to the increased oxygen requirement of the proliferating cancer cells and the poor blood supply.[8] The induction of VEGF in the hypoxic condition is mediated by a transcription factor, hypoxia-inducible factor 1 (HIF1), a heterodimeric complex of HIF1α and HIF1β subunits. HIF1α is easily degraded under normoxic conditions, but becomes stable under hypoxic conditions, and makes a heterodimeric complex with HIF1β. The dimer binds to the hypoxia responsive element in the promoter of the VEGF gene.[9] A worse prognosis in patients with NSCLC is associated with increased expression of HIF1 in cancer cells.[10] Fibroblast growth factor (FGF)-2 is another growth factor that has potent angiogenic activity. The induction of FGF-2 in cancer cells is also associated with the angio-

Supported by a Grant-in-Aid for Scientific Research on Priority Areas from the Japanese Ministry of Education, Science, Sports and Culture, and by Health and Labor Sciences research grants, Third Term Comprehensive Control Research for Cancer, from the Ministry of Health, Labor, and Welfare (Japan).

Accepted for publication March 26, 2009.

Present Address of Takuya Moriya: Department of Pathology, Kawasaki Medical School Hospital, 577 Matsushima, Kurashiki 701-0192, Japan.

Address reprint requests to Yasufumi Sato, Department of Vascular Biology, Institute of Development, Aging and Cancer, Tohoku University, 4-1, Seiryo-machi, Aoba-ku, Sendai 980-8575, Japan. E-mail: y-sato@idac.tohoku.ac.jp.

Table 1. Patient Profile

Number of patients	44
Sex (%)	
Male	28 (63.6)
Female	16 (36.4)
Age	
Mean (range)	66.2 (45–82)
Histology (%)	
Adenocarcinoma	35 (79.5)
Squamous cell carcinoma	9 (20.5)
Stage (%)	
IA	29 (65.9)
IB	5 (11.3)
IIA	0 (0)
IIB	1 (2.3)
IIIA	7 (15.9)
IIIB	1 (2.3)
IV	1 (2.3)

genic switch.[11] Indeed, FGF-2 is expressed in some NSCLC cells.[5–7]

The activities of angiogenesis stimulators are normally countered by angiogenesis inhibitors. A number of angiogenesis inhibitors have been identified to date.[12] Thrombospondin 1 is the best-characterized angiogenesis inhibitor in NSCLC. The expression of thrombospondin 1 is under the control of p53.[13] In cancer cells including NSCLC, alteration of the p53 gene is associated with decreased expression of thrombospondin 1.[14] The decreased expression of thrombospondin 1 in NSCLC is confirmed by others,[15–17] and correlates with poor prognosis.[15]

We have recently isolated a novel angiogenesis inhibitor, vasohibin (VASH), from endothelial cells (ECs).[18] Because a homologue of VASH was reported as

Table 2. Relationship between VEGF and HIF-1α in NSCLCs

	VEGF Negative	VEGF Positive	Total
HIF-1α Negative	9	2	11
HIF-1α Positive	12	21	33
Total	21	23	44

VASH2,[19] the prototype VASH is now called VASH1. The characteristic feature of VASH1 is that it is induced in ECs by VEGF and FGF-2, two potent angiogenic factors.[18,20] Here we characterize the significance of VASH1 in tumors. We first verify the localization of VASH1 in relation to HIF1α, VEGF, or FGF-2 in the pathological sections of NSCLC. We then evaluate the role of VASH1 in tumor angiogenesis in animal models. Our analysis reveals that endogenous VASH1 is expressed in ECs of tumor blood vessels, and it is involved in the termination of tumor angiogenesis. When applied exogenously, VASH1 inhibits sprouting angiogenesis in tumors, matures the remaining vessels, and enhances the antitumor effect of chemotherapy.

Materials and Methods

Materials

We used the following materials: anti-human CD31 monoclonal antibody (mAb), anti-human α-smooth muscle actin (αSMA) mAb, and Rabbit/Mouse Ig Immunohistochemistry Kit (DAKO Cytomation, Glostrup, Denmark); anti-human HIF-1α goat antibody (Ab), and anti-human

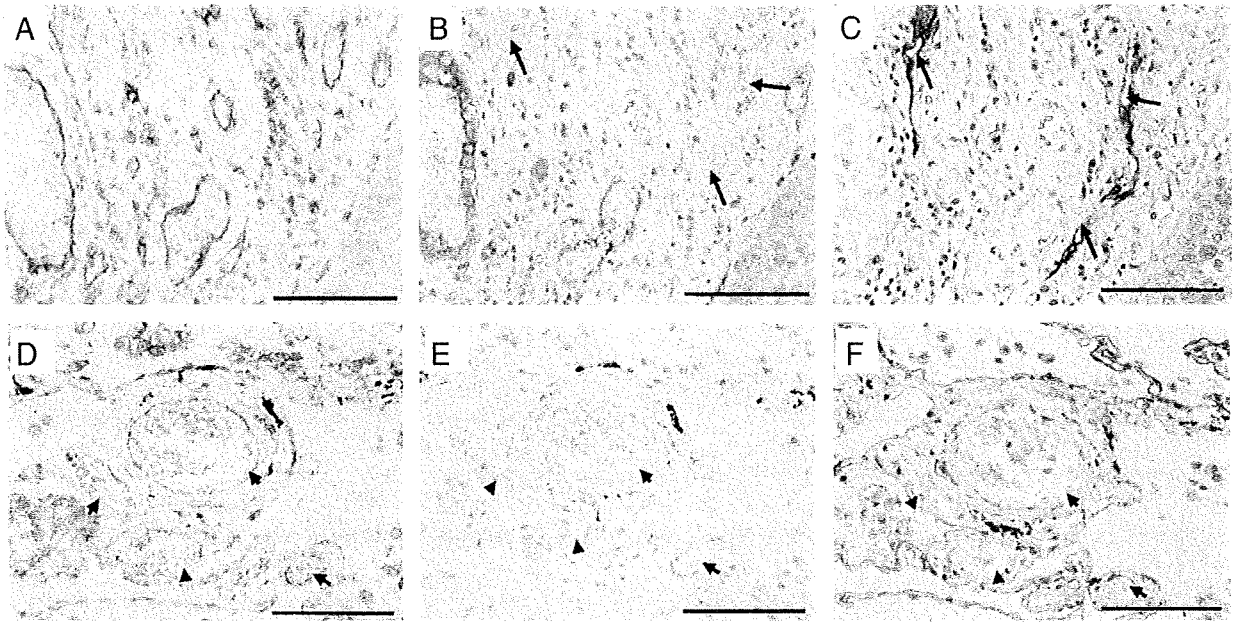

Figure 1. Presence of VASH1 in blood vessel ECs in the tumor stroma of NSCLCs. Pathological sections of NSCLC were immunostained for endothelial cell marker CD31 (**A** and **D**), VASH1 (**B** and **E**), and the lymphatic endothelial cell marker podoplanin (**C** and **F**). (**A**), (**B**) and (**C**) show tumor stroma, whereas (**D**), (**E**), and (**F**) show non-cancerous region in the same patient. Scale bar = 100 μm. VASH1 was present in blood vessel ECs in the tumor stroma of NSCLCs. **Arrows** indicate lymphatic vessels in tumor stroma and **arrowheads** indicate blood vessels in non-cancerous resion.

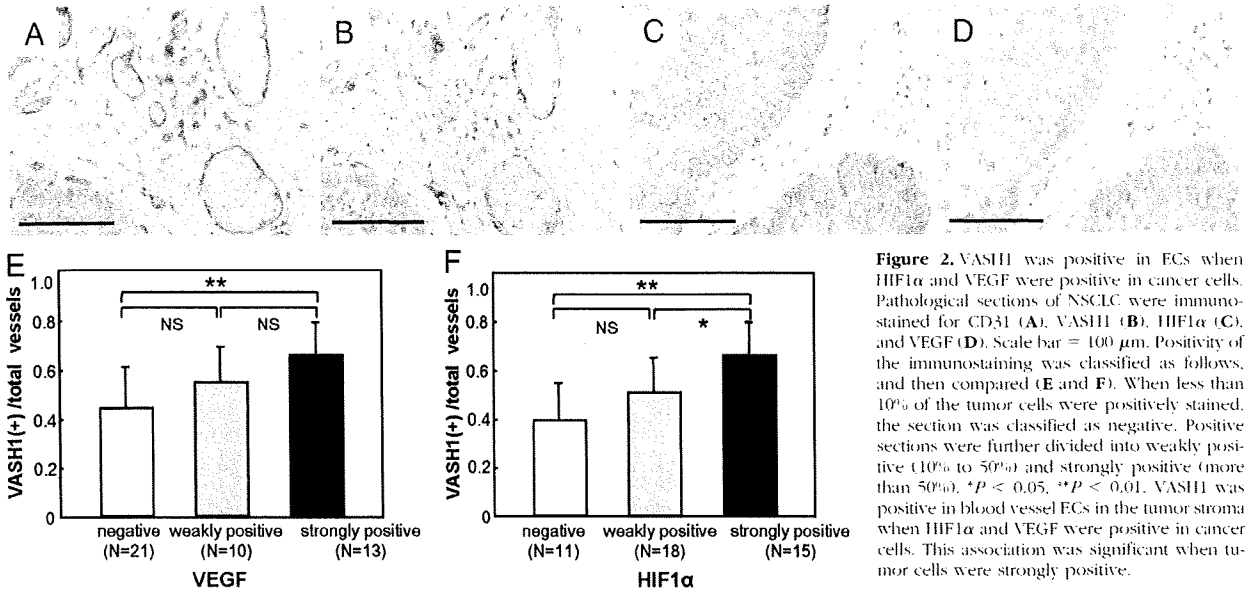

Figure 2. VASH1 was positive in ECs when HIF1α and VEGF were positive in cancer cells. Pathological sections of NSCLC were immunostained for CD31 (**A**), VASH1 (**B**), HIF1α (**C**), and VEGF (**D**). Scale bar = 100 μm. Positivity of the immunostaining was classified as follows, and then compared (**E** and **F**). When less than 10% of the tumor cells were positively stained, the section was classified as negative. Positive sections were further divided into weakly positive (10% to 50%) and strongly positive (more than 50%). $^{*}P < 0.05$, $^{**}P < 0.01$. VASH1 was positive in blood vessel ECs in the tumor stroma when HIF1α and VEGF were positive in cancer cells. This association was significant when tumor cells were strongly positive.

FGF-2 rabbit Ab (Santa Cruz Biotechnology, Santa Cruz, CA); anti-human podoplanin mAb (AngioBio, Del Mar, CA); anti-human VEGF mAb (LAB VISION, Fremont, CA); anti-human β-actin mAb, anti-mouse αSMA mAb, horseradish peroxidase-conjugated anti-mouse IgG and *cis*-diammineplatinum dichloride (CDDP) (Sigma, St. Louis, MO); anti-mouse CD31 rat Ab (Fitzgerald Industries International, Concord, MA); anti-mouse platelet-derived growth factor receptor β goat Ab (R&D Systems, Minneapolis, MN); biotin-conjugated anti-mouse or anti-goat IgG, IgA, IgM Ab, and streptavidin-biotin peroxidase complex (Nichirei Biosciences, Tokyo, Japan); Alexa fluor 568 labeled goat anti-rat IgG; Alexa 488 labeled donkey anti-mouse IgG; Alexa 488 labeled donkey anti-goat IgG; TO-PRO-3 iodide (Molecular Probes, Eugene, OR); OCT compound (Sakura Finetechnical, Tokyo, Japan); Dulbecco's modified Eagle's Medium (Nissui Pharmaceutical Co., Tokyo, Japan); fetal bovine serum (Equitech-Bio, Kerrville, TX); and diaminobenzidine (Sigma). Anti-human vasohibin-1 (VASH1) mAb was described previously.[18]

Patients

The clinical study included 44 patients with NSCLC, who underwent partial resection of a lung (lobectomy or pneumonectomy) in Tohoku University Hospital between November 2003 and January 2007. Informed consents were obtained from all of the patients, and the study was approved by the Ethical Committee of Tohoku University.

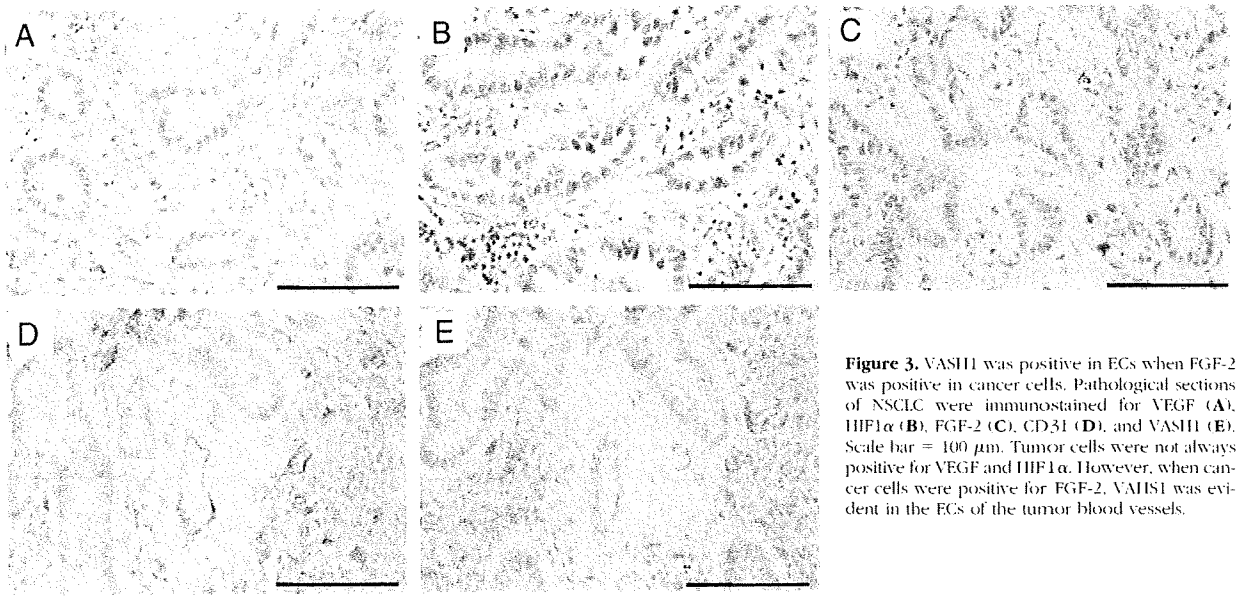

Figure 3. VASH1 was positive in ECs when FGF-2 was positive in cancer cells. Pathological sections of NSCLC were immunostained for VEGF (**A**), HIF1α (**B**), FGF-2 (**C**), CD31 (**D**), and VASH1 (**E**). Scale bar = 100 μm. Tumor cells were not always positive for VEGF and HIF1α. However, when cancer cells were positive for FGF-2, VASH1 was evident in the ECs of the tumor blood vessels.

Table 3. Relationship between VEGF and FGF-2 in NSCLCs

	VEGF Negative	VEGF Positive	Total
FGF-2 Negative	15	3	18
FGF-2 Positive	6	20	26
Total	21	23	44

Immunohistochemical Analysis of Human Lung Specimens

Human lung specimens were fixed in 10% formalin, embedded in paraffin, and cut into 3-μm thick sections. Sections were dewaxed in xylene, rehydrated in a graded ethanol series (100%, 90%, 80%, and 70%), and incubated in 10% H_2O_2/methanol to block endogenous peroxidase activity. Sections were then incubated in citrated buffer (pH 6.0) for 5 minutes at 121°C in a microwave oven for VASH1, CD31, and FGF-2 staining, in citrated buffer (pH 6.0); in the same conditions for 15 minutes for VEGF staining; and in 0.1% Trypsin/0.05 mol/L Tris buffer (pH 7.6) for 30 minutes at 37°C for αSMA staining. Thereafter, sections were incubated for 10 minutes at room temperature in a blocking solution of 10% rabbit or goat serum (Nichirei Biosciences). Primary antibody reactions were performed overnight at 4°C at a dilution of 1:400 for anti-human VASH1 mAb, 1:40 for anti-human CD31 mAb, 1:800 for anti-human αSMA mAb, 1:100 for anti-human HIF1α goat Ab, 1:200 for anti-human podoplanin mAb, 1:50 for anti-human VEGF mAb, and 1:200 for anti-FGF-2 rabbit Ab. A secondary antibody reaction was performed with biotin-conjugated anti-mouse or anti-goat IgG, IgA, and IgM Ab for 30 minutes at room temperature. Streptavidin-biotin peroxidase complex formation was performed for 30 minutes at room temperature. Sections were visualized using diaminobenzidine/H_2O_2 and sodium azide in 0.05mol/L Tris buffer, (pH 7.6). Nuclei were counterstained with hematoxylin.

To localize VASH1, mirror sections were prepared. One section was stained for CD31 and αSMA, and the other was stained for VASH1. For CD31 and αSMA, primary antibody reactions were performed overnight at 4°C; for anti-human CD31 mAb reactions were performed at day one. On day 2, sections were visualized using diaminobenzidine, 0.1 M/L glycine buffer (pH 2.2) for 30 minutes at room temperature. After treatment in 0.1% Trypsin, 0.05 mol/L Tris buffer, pH7.6, for 30 minutes at 37°C and washing with PBS three times, the sections underwent the primary antibody reaction for anti-human αSMA mAb overnight at 4°C. On day three, sections were visualized using 4 chloro-1naphtol and ethanol, 0.05 mol/L Tris buffer (pH 7.6)/H_2O_2, for 30 minutes at room temperature. After being washed with PBS three times, the sections were covered with aqueous mounting medium.

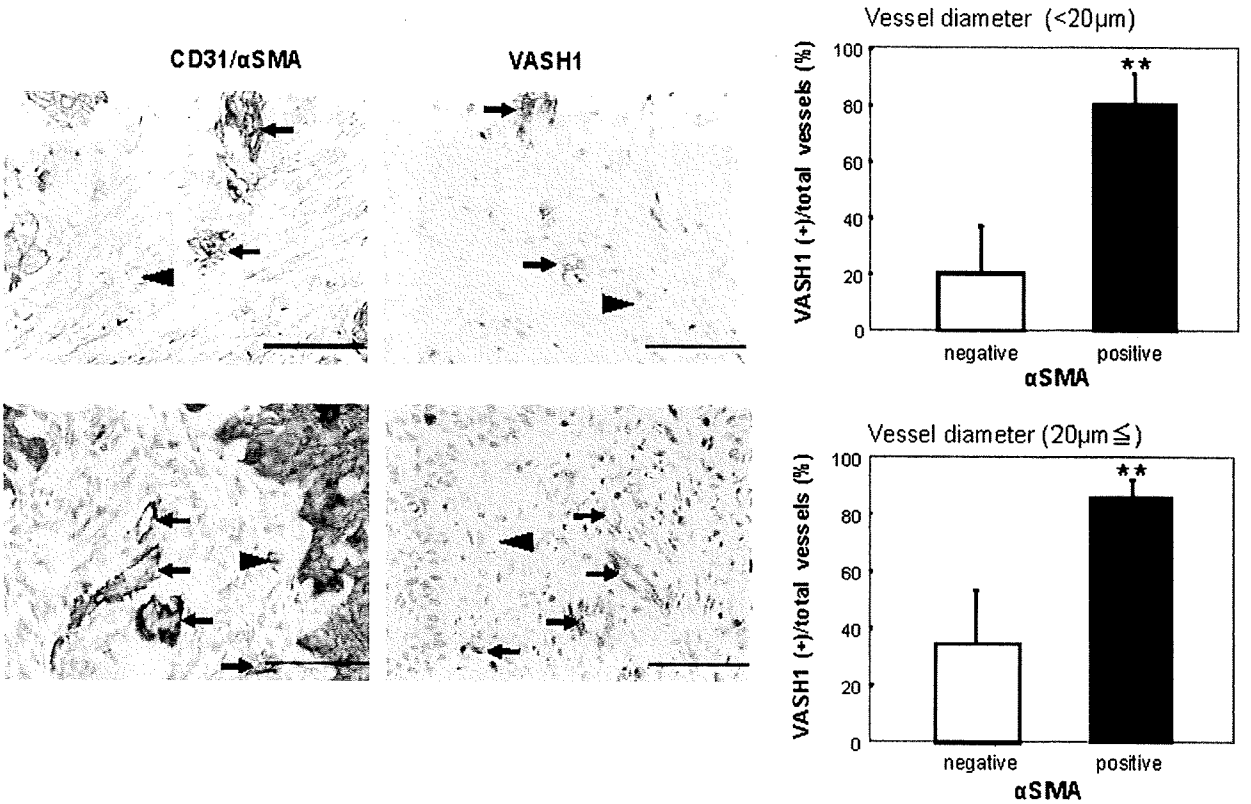

Figure 4. VASH1 was positive in ECs of tumor vessels when they were associated with mural cells. Mirror sections of NSCLC were immunostained for CD31 (brown) and αSMA (purple) on the left, and VASH1 (brown) on the right. Scale bar = 100 μm. VASH1 was positive when the vessels were associated with mural cell (**arrows**). VASH1 was negative when the vessel was not associated with mural cell (**arrowheads**). Quantification revealed that the positivity of VASH1 with mural cell association was evident regardless of the size of blood vessels. $^{**}P < 0.01$.

Interpretation of the Immunohistochemical Staining

Two pathologists evaluated all of the slides independently. To analyze CD31 and VASH1 staining, slides were scanned at low magnification (×100), and then vessels were counted in four random intratumoral areas of 1 mm^2, and in four random peritumoral areas of 1 mm^2. To determine HIF-1α, VEGF, and FGF-2 staining, slides were scanned at low magnification (×100). When less than 10% of the tumor cells were positively stained, the section was classified as negative; when more than 10% were positively stained, the section was classified as positive. In some cases, positive sections were further divided in to weakly positive (10% to 50%) and strongly positive (more than 50%).

Cells

Lewis lung carcinoma (LLC) cells were cultured in Dulbecco's modified Eagle's Medium supplemented with 10% fetal bovine serum, 100 μg/ml penicillin, 100 μg/ml streptomycin, and 4 mmol/L L-glutamine.[21]

Tumor Growth in Mice

Male C57 BJ/6 J mice, 6 to 8-week-old (Charles River, Japan) or *VASH1*$^{-/-}$ mice of C57 BJ/6 background[22]

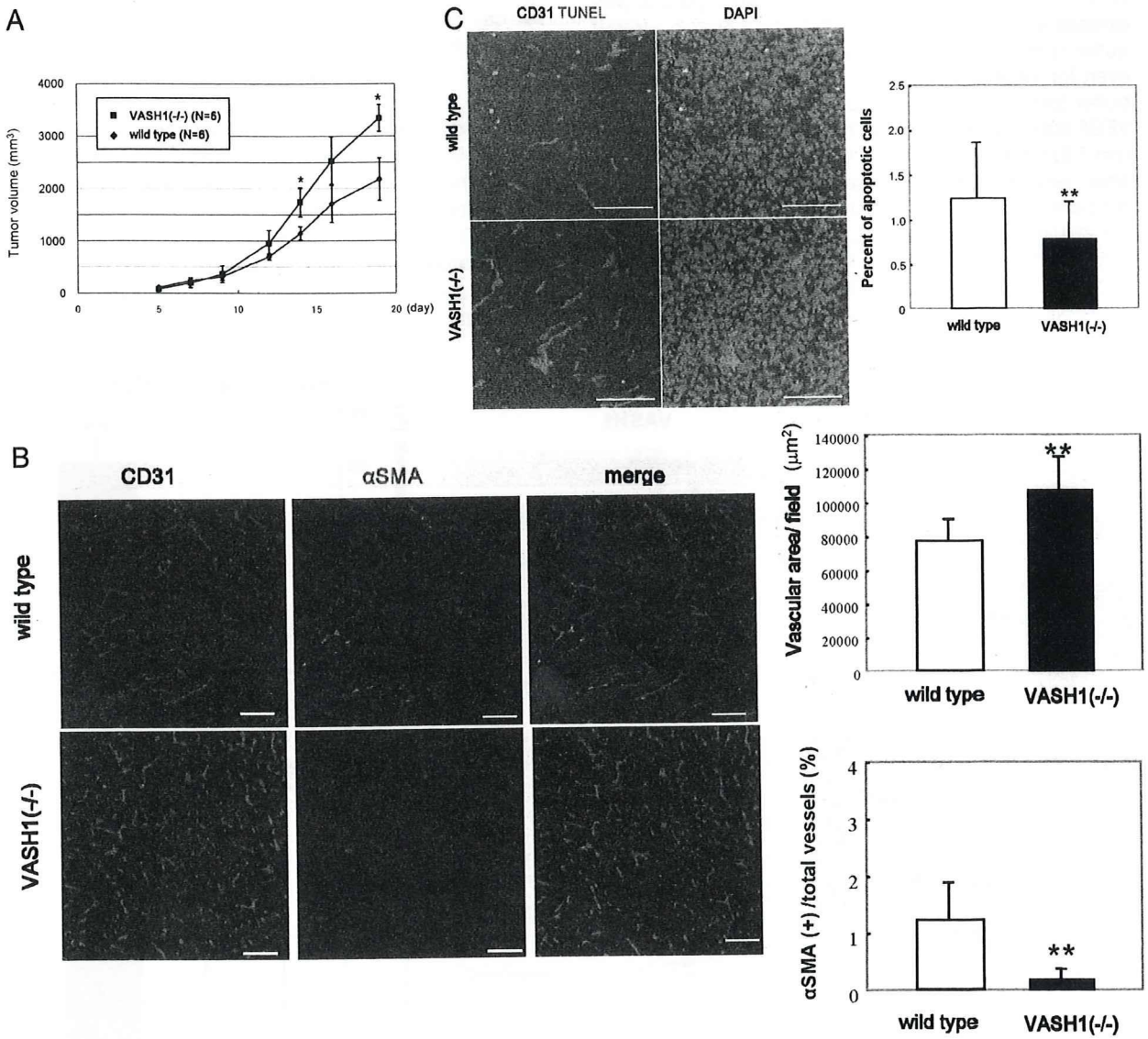

Figure 5. Tumor growth and tumor angiogenesis in *VASH1*$^{-/-}$ mice. **A:** LLC cells (5×10^6) were inoculated in wild-type and *VASH1*$^{-/-}$ mice, and tumor growth was evaluated. Data are expressed as the means and SDs. Tumors in *VASH1*$^{-/-}$ mice tended to grow bigger. $^*P < 0.05$. **B:** Tumor sections were co-immunostained for CD31 and αSMA. Tumors in *VASH1*$^{-/-}$ mice contained numerous small vessels. Scale bar = 100 μm. For this analysis, we counted 221 to 444 vessels per field (357 ± 66 per field) in wild-type and 328 to 780 vessels per field (472 ± 129 per field) in knockout mice. Quantification revealed that the vascularized tumor area in *VASH1*$^{-/-}$ mice was significantly increased, and vessels in *VASH1*$^{-/-}$ mice were more immature. $^{**}P < 0.01$. **C:** Apoptosis was evaluated by terminal deoxynucleotidyl transferase dUTP nick-end labeling. Scale bar = 100 μm. Tumors in *VASH1*$^{-/-}$ contained fewer apoptotic tumor cells. $^{**}P < 0.01$.

were inoculated in the subcutaneous tissue of the right abdominal wall with 5×10^6 LLC cells. Every 2 days after the inoculation, perpendicular tumor diameters were measured by digital calipers, and the tumor volume was calculated as $0.5 \times \text{length} \times \text{width}^2$. At indicated periods after the inoculation, mice were sacrificed, and tumors were collected.

To evaluate the effect of VASH1, we used a replication-defective adenovirus vector encoding the human *VASH1* gene (AdVASH1). A replication-defective adenovirus vector encoding the *β-galactosidase* gene (AdLacZ) was used for the control.[18,23] A total of 100 μl AdVASH1 or AdLacZ, containing 1×10^9 plaque-forming units were injected into the mouse tail vein on day 7 after the inoculation. For the combination with CDDP, AdVASH1 or AdLacZ was injected in the tail vein at day 6 after the inoculation. The mice were then given an intraperitoneal injection of CDDP (2.5 mg/kg) on days 10, 14, and 18.[24,25]

Tumor tissues were embedded in OCT compound to make frozen tissue specimens, and sectioned at 7 μm. Sections were fixed with methanol for 20 minutes at 20°C, blocked with Protein Block Serum Free (DAKO Cytomation) for 10 minutes at room temperature, and stained with anti-mouse CD31 rat Ab (1:200), anti-mouse α-SMA mAb (1:200) or anti-mouse platelet-derived growth factor receptor (PDGFR) β goat Ab (1:10) overnight, followed by staining with Alexa fluor 568 labeled goat anti-Rat IgG (1:400), Alexa 488 labeled donkey anti-mouse IgG (1:400), Alexa 488 labeled donkey anti-goat IgG (1:400), and TO-PRO-3 iodide (1:1000) for 60 minutes at room temperature. After being washed with PBS three times, the sections were covered with fluorescent mounting medium. Terminal deoxynucleotidyl transferase dUTP nick-end labeling staining used Fluorescein FragEL DNA Fragmentation Detection Kit (EMD Chemicals Inc., Darmstadt, Germany) following manufacturer protocols. Stained samples were visualized using an Olympus FluoView FV1000 confocal microscope (Tokyo, Japan). The vascular lumen was traced and the luminal area was analyzed with NIH ImageJ software.

Statistical Analysis

Data are expressed as mean ± SD The statistical significance of differences was evaluated using the

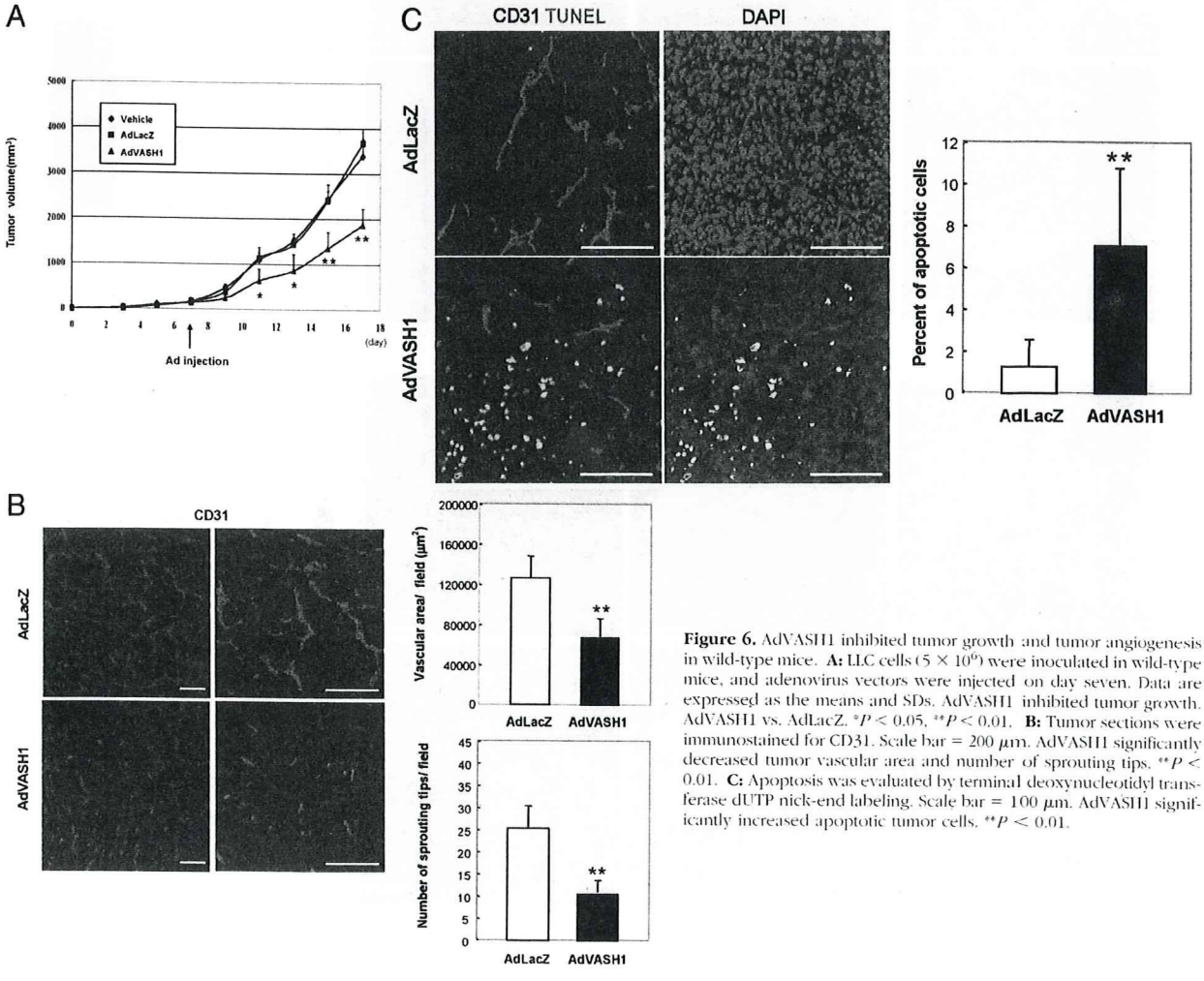

Figure 6. AdVASH1 inhibited tumor growth and tumor angiogenesis in wild-type mice. **A:** LLC cells (5×10^6) were inoculated in wild-type mice, and adenovirus vectors were injected on day seven. Data are expressed as the means and SDs. AdVASH1 inhibited tumor growth. AdVASH1 vs. AdLacZ. $^*P < 0.05$, $^{**}P < 0.01$. **B:** Tumor sections were immunostained for CD31. Scale bar = 200 μm. AdVASH1 significantly decreased tumor vascular area and number of sprouting tips. $^{**}P < 0.01$. **C:** Apoptosis was evaluated by terminal deoxynucleotidyl transferase dUTP nick-end labeling. Scale bar = 100 μm. AdVASH1 significantly increased apoptotic tumor cells. $^{**}P < 0.01$.

unpaired analysis of variance (analysis of variance), and P values were calculated using the unpaired Student's t-test. A value of $P < 0.05$ was accepted as statistically significant.

Results

Presence of VASH1 in Blood Vessel ECs in the Tumor Stroma of NSCLCs

We first evaluated the presence of VASH1 protein in human NSCLC specimens. The study included 44 patients with NSCLC (28 males and 16 females). Their average age was 66.2 years (range, 45 to 82 years). Based on the World Health Organization's criteria for tumor types, 35 patients had adenocarcinomas, and nine had squamous cell carcinomas. Twenty-nine patients had stage IA cancers, five patients had stage IB, one had stage II, eight had stage III, and one had stage IV cancers (Table 1).

Pathological sections of NSCLC were analyzed as follows. VASH1 was present in CD31 positive ECs, which were negative for lymphatic EC marker podoplanin (Figure 1A, C, D, and F). Thus, VASH1 is preferentially expressed in ECs of blood vessels. VASH1 was evident only in the tumor stroma (Figure 1B), and not in the non-cancerous region of the surgically resected tissue of the same patient (Figure 1E). This distinction indicates that the expression of this protein is closely associated with tumor blood vessels.

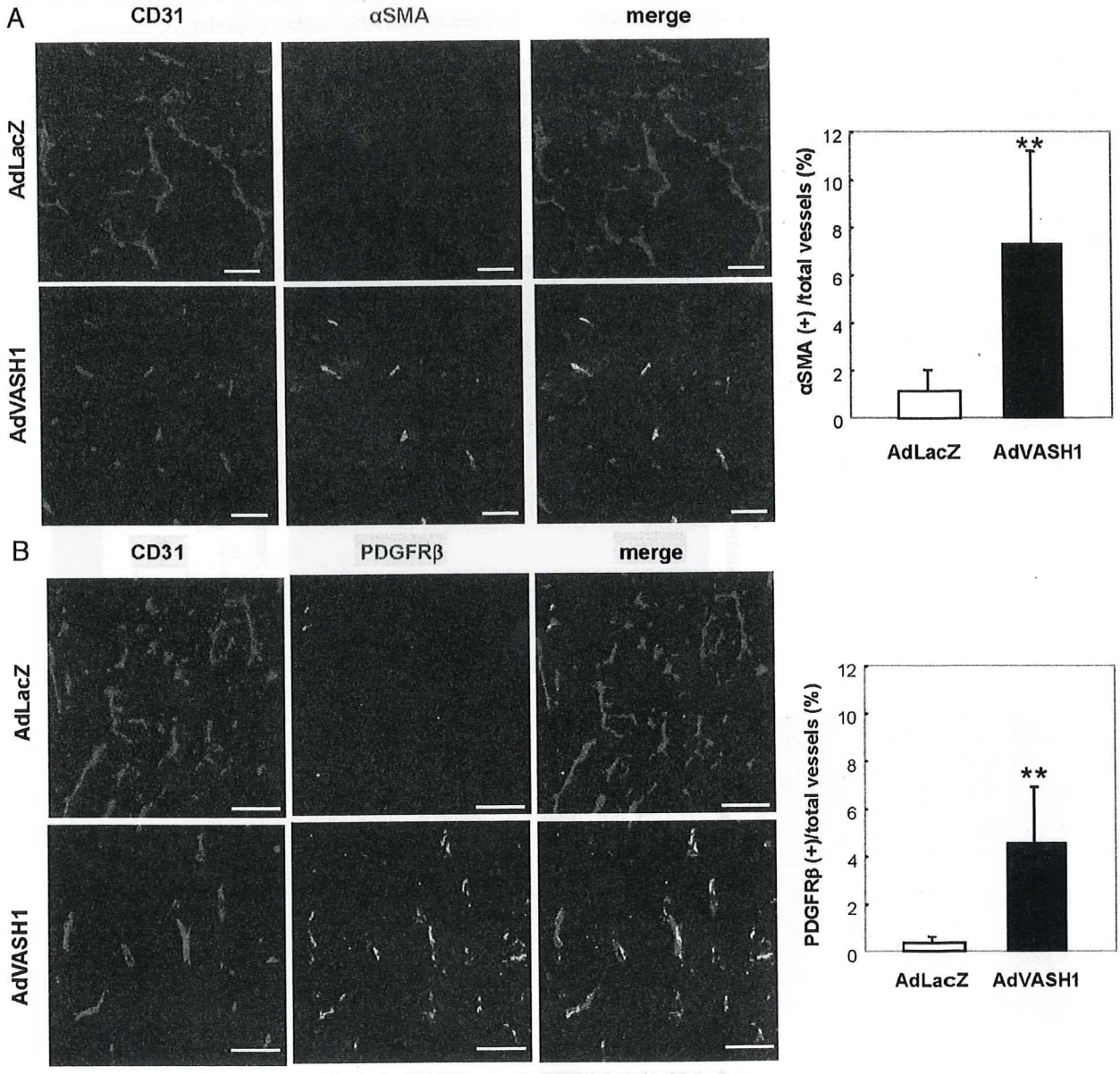

Figure 7. AdVASH1 matured tumor vessels in wild-type mice. Tumor sections were co-immunostained for (**A**) CD31 and αSMA or CD31 and (**B**) PDGFR β, an additional marker of mural cells. Scale bar = 100 μm. Tumor vessels in AdVASH1 injected mice were more frequently associated with mural cells. $^{**}P < 0.01$.

Relationship between VASH1 in ECs and VEGF or FGF-2 in Cancer Cells

Because VASH1 was inducible by two representative angiogenic factors, VEGF and FGF-2, in ECs,[18,20] we evaluated the relationships between VASH1 and VEGF or FGF-2. Because VEGF is induced in hypoxic conditions, the presence of VEGF was associated with the presence of HIF1α in cancer cells (Table 2).[26] Immunohistochemical analysis revealed that VASH1 was present in ECs in tumor blood vessels (Figure 2, A and B) when NSCLC cells were positive for VEGF and HIF-1α (Figure 2, C and D). Quantitative analysis confirmed that the presence of VASH1 in ECs was significantly higher in both VEGF positive and HIF1α positive tumors (Figure 2, E and F).

FGF-2 is another potent angiogenic factor. NSCLC cells were not always positive for VEGF. However, when cancer cells were positive for FGF-2, VASH1 was present in the ECs of tumor blood vessels (Figure 3A–E). The relationship between VEGF and FGF-2 is shown in Table 3.

Association of VASH1-Positive Tumor Vessels with Mural Cells

As we noticed that not all of the tumor blood vessels were positive for VASH1, we determined the characteristics of VASH1-positive tumor blood vessels. Immunostaining of αSMA in the mirror sections of NSCLC revealed that VASH1 was preferentially expressed in ECs when tumor blood vessels were associated with mural cells (Figure 4). Quantitative analysis further confirmed this association, independent of the sizes of the blood vessels (Figure 4).

Tumor Vessels in VASH1$^{-/-}$ Mice

The presence of endogenous VASH1 in tumor vessels promoted us to evaluate the function of this molecule in the animal model. When LLC cells were inoculated in *VASH1*$^{-/-}$ mice, tumors in *VASH1*$^{-/-}$ mice tended to grow bigger than in wild-type mice (Figure 5A). We then evaluated tumor vessels in *VASH1*$^{-/-}$ mice. The vascular area was increased and tumor vessels were more immature lacking mural cells in *VASH1*$^{-/-}$ mice (Figure 5B). Although the number of apoptotic cancer cells in wild-type mice was at a rather low level, it was further decreased in *VASH1*$^{-/-}$ mice (Figure 5C). These results indicate that endogenous VASH1 does function as an angiogenesis inhibitor in tumors.

Effect of Exogenous VASH1 on Tumor Growth and Tumor Angiogenesis

We next examined the effect of exogenous VASH1. We inoculated LLC cells into wild-type mice, and injected AdVASH1 in the tail vein 7 days later. This procedure supplies sufficient VASH1 protein to regulate angiogenesis as described previously.[23] AdLacZ was used as a negative control.[23] AdVASH1 injection significantly inhibited the growth of tumor in mice (Figure 6A). The immunohistochemical analysis revealed that the tumor vascular area was decreased and tumor cell apoptosis was augmented in the AdVASH1-treated mice (Figure 6, B and C). Moreover, the remaining tumor vessels in the AdVASH1-treated mice were small, round, and mature, associating with mural cells; whereas tumor vessels in the control AdLacZ-injected mice were dilated, erratic, and immature, containing sprouting endothelial cells with few mural cells (Figure 7, A and B).

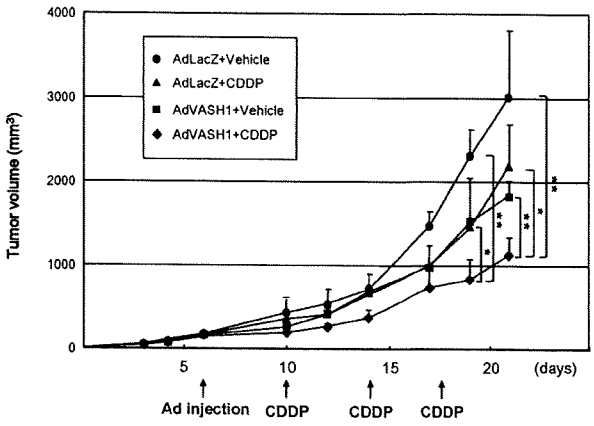

Figure 8. Anti-tumor activity of CDDP was enhanced when combined with AdVASH1. LLC cells (5×10^6) were inoculated in wild-type mice. Adenovirus vectors were injected on day seven, and CDDP (2.5 mg/kg) was injected on days 10, 14, and 18. Data are expressed as the means and SDs. AdVASH1 injection improved the anti-tumor effect of CDDP. $^{*}P < 0.05$, $^{**}P < 0.01$.

Because the VASH1 treatment caused the remaining tumor vessels to mature, we anticipated that those vessels would deliver anti-cancer drugs efficiently. We therefore tested the efficacy of the combination of VASH1 with CDDP. As expected, AdVASH1 injection improved the anti-tumor effect of CDDP (Figure 8).

Discussion

The search for molecular biomarkers of angiogenesis has been intensively pursued. Molecules that are specifically expressed in ECs can be candidates for such biomarkers. CD31, von Willebrand factor, and vascular endothelial-cadherin are used for histological identification of ECs.[27] However, those molecules are expressed in quiescent ECs as well, and thus cannot be specific for active angiogenesis. Endoglin and aminopeptidase N are expressed preferentially in ECs during angiogenesis.[28,29] Therefore, these two molecules are more suitable markers of angiogenesis. Additionally, several attempts have been made to isolate molecules that are expressed in cancer-specific ECs.[30–32] Nevertheless, such molecules had not been characterized in the clinical setting. In this report, we characterized the significance of VASH1, a VEGF-inducible angiogenesis inhibitor, in NSCLCs. Our data reveal that the expression of VASH1 was restricted to ECs of blood vessels in the tumor stroma, and was correlated with the expression of HIF-1α and VEGF, or FGF-2 in tumor cells. We have previously showed the presence of VASH1 in tumor vessels of human endome-

trial cancers as well.[33] We therefore propose that VASH1 should be further tested as a candidate of tumor angiogenesis biomarker.

We have previously determined the role of VASH1 in the mouse subcutaneous angiogenesis model.[22] Angiogenesis is normally synchronized and transient, as hypoxia-mediated angiogenic stimuli withdraw when blood starts to flow in the newly formed vessels. Our previous analysis in the mouse subcutaneous angiogenesis model has revealed that endogenous VASH1 is present in newly formed blood vessels behind the sprouting front where angiogenesis terminates (termination zone), and those VASH1-positive vessels are mature associated with mural cells.[22] As cancers contain complex lesions where angiogenesis is not synchronized and sprouting occurs randomly, it is difficult to dissect the spatio-temporal expression pattern of VASH1 in cancers. Here we show that VASH1 is prevalent in tumor blood vessels of NSCLC when they are associated with mural cells (Figure 4). This result suggests that the spatio-temporal expression profile of VASH1 is maintained even in tumor vessels.

Increased expression of angiogenesis stimulators, together with decreased expression of angiogenesis inhibitors, is proposed to occur in various cancers.[34] The presence of VASH1 in tumor vessels thus raises the question whether endogenous VASH1 acts as an angiogenesis inhibitor in tumors. We have previously demonstrated in the mouse subcutaneous angiogenesis model that the function of endogenous VASH1 is to terminate angiogenesis, but is not to inhibit angiogenesis in the sprouting front.[22] Here we compared tumors in wild-type and *VASH1*$^{-/-}$ mice. Tumors growth in wild-type mice was slower than in *VASH1*$^{-/-}$ mice. Histological analysis further demonstrated the distinction that tumors in *VASH1*$^{-/-}$ mice contained more immature vessels and fewer apoptotic tumor cells. This observation indicates that endogenous VASH1 does participate in the inhibition of tumor angiogenesis.

The persistence of sprouting ECs in tumor vessels in wild-type mice implies that endogenous VASH1 is ineffective in blocking sprouting angiogenesis in tumors. Importantly, when sufficient VASH1 is supplied exogenously, it can block angiogenesis in the sprouting front.[22] Here we show that sprouting ECs disappear from tumor vessels by the injection of AdVASH1. Tumor vessels in the control AdLacZ-injected mice were dilated, erratic and immature, containing fewer mural cells, whereas those in the AdVASH1-treated mice were small, round, and mature, associated with mural cells. These morphological differences imply that exogenous VASH1 has two modalities affecting tumor vessels. One is to inhibit sprouting angiogenesis, and the other is to participate in the termination of angiogenesis.

Abnormal tumor vessels bring about deficient blood flow within the tumor, which should impair the delivery of drugs to the tumor.[35] Maturation of tumor vasculature enhances the efficacy of cytotoxic anti-cancer therapies, as it increases the delivery of anti-cancer drugs to the tumor cells.[35] We therefore anticipated that exogenous VASH1 should enhance the efficacy of cytotoxic anti-cancer therapies. Indeed, the combination of AdVASH1 with CDDP did improve its efficacy.

In summary, VASH1 is selectively expressed in the ECs of tumor blood vessels. The expression is related to expression of angiogenic factors such as VEGF and FGF-2, and thus VASH1 can be further evaluated as an angiogenesis biomarker. Expression of endogenous VASH1 may participate in the inhibition of tumor angiogenesis, although it is not enough to block sprouting. However, exogenous VASH1 effectively inhibits sprouting angiogenesis, matures tumor vessels, and enhances antitumor efficacy when combined with conventional chemotherapy. We propose that VASH1 should be further tested in cancer diagnosis and therapy.

Acknowledgments

We thank Yuriko Fujinoya and Kyoko Shimizu for their excellent technical assistance.

References

1. Yano S, Matsumori Y, Ikuta K, Ogino H, Doljinsuren T, Sone S: Current status and perspective of angiogenesis and antivascular therapeutic strategy: non-small cell lung cancer. Int J Clin Oncol 2006, 11:73–81
2. Jain RK: Lessons from multidisciplinary translational trials on anti-angiogenic therapy of cancer. Nat Rev Cancer 2008, 8:309–316
3. Stinchcombe TE, Socinski MA: Bevacizumab in the treatment of non-small-cell lung cancer. Oncogene 2007, 26:3691–3698
4. Ferrara N, Kerbel RS: Angiogenesis as a therapeutic target. Nature 2005, 438:967–974
5. Bremnes RM, Camps C, Sirera R: Angiogenesis in non-small cell lung cancer: the prognostic impact of neoangiogenesis and the cytokines VEGF and bFGF in tumours and blood. Lung Cancer 2006, 51:143–158
6. Mattern J, Koomagi R, Volm M: Association of vascular endothelial growth factor expression with intratumoral microvessel density and tumour cell proliferation in human epidermoid lung carcinoma. Br J Cancer 1996, 73:931–934
7. Takanami I, Imamura T, Hashizume T, Kikuchi K, Yamamoto Y, Yamamoto T, Kodaira S: Immunohistochemical detection of basic fibroblast growth factor as a prognostic indicator in pulmonary adenocarcinoma. Jpn J Clin Oncol 1996, 26:293–297
8. Carmeliet P: VEGF as a key mediator of angiogenesis in cancer. Oncology 69 Suppl 2005, 3:4–10
9. Liao D, Johnson RS: Hypoxia: a key regulator of angiogenesis in cancer. Cancer Metastasis Rev 2007, 26:281–290
10. Swinson DE, O'Byrne KJ: Interactions between hypoxia and epidermal growth factor receptor in non-small-cell lung cancer. Clin Lung Cancer 2006, 7:250–256
11. Kandel J, Bossy-Wetzel E, Radvanyi F, Klagsbrun M, Folkman J, Hanahan D: Neovascularization is associated with a switch to the export of bFGF in the multistep development of fibrosarcoma. Cell 1991, 66:1095–1104
12. Sato Y: Update on endogenous inhibitors of angiogenesis. Endothelium 2006, 13:147–155
13. Dameron KM, Volpert OV, Tainsky MA, Bouck N: Control of angiogenesis in fibroblasts by p53 regulation of thrombospondin-1. Science 1994, 265:1582–1584
14. Fontanini G, Boldrini L, Calcinai A, Chine S, Lucchi M, Mussi A, Angeletti CA, Basolo F, Bevilacqua G: Thrombospondins I and II messenger RNA expression in lung carcinoma: relationship with p53 alterations, angiogenic growth factors, and vascular density. Clin Cancer Res 1999, 5:155–161
15. Yamaguchi M, Sugio K, Ondo K, Yano T, Sugimachi K: Reduced expression of thrombospondin-1 correlates with a poor prognosis in